1 **Morphodynamics of boulder-bed semi-alluvial streams in northern Fennoscandia: a**
2 **flume experiment to determine sediment self-organization**

3

4 **L. E. Polvi[1]**

5 [1]Department of Ecology & Environmental Science, Umeå University, Umeå, 907 36 Sweden

6 Corresponding author: Lina E. Polvi (lina.polvi@umu.se)

7

8 **Key Points:**

9 • Boulder-bed semi-alluvial channels behave like low submergence regime mountain
10 streams with sediment deposition upstream of boulders

11 • Fennoscandian semi-alluvial rapids are not re-worked (boulders transported or bedform
12 formation) by high fluvial flows (i.e., Q_{50})

13 • Large grains ($>D_{84}$) are important in shaping channel morphodynamics and have
14 implications for restoration of salmonid spawning gravel

15

16 **Abstract**

17   In northern Fennoscandia, semi-alluvial boulder-bed channels with coarse glacial legacy
18 sediment are abundant, and due to widespread anthropogenic manipulation during timber-
19 floating, unimpacted reference reaches are rare. The landscape context of these semi-alluvial
20 rapids— with numerous mainstem lakes that buffer high flows and sediment connectivity in
21 addition to a regional low sediment yield— contribute to low amounts of fine sediment and
22 incompetent flows to transport boulders. To determine the morphodynamics of semi-alluvial
23 rapids and potential self-organization of sediment with multiple high flows, a flume experiment
24 was designed and carried out to mimic conditions in semi-alluvial rapids in northern
25 Fennoscandia. Two slope setups (2% and 5%) were used to model a range of flows (Q_1 (summer
26 high flow), Q_2, Q_{10} & Q_{50}) in a 8 x 1.1 m flume with a sediment distribution analogous to field
27 conditions; bed topography was measured using structure-from-motion photogrammetry after
28 each flow to obtain DEMs. No classic steep coarse-bed channel bedforms (e.g., step-pools)
29 developed. However, similarly to boulder-bed channels with low relative submergence, at Q_{10}
30 and Q_{50} flows, sediment deposited upstream of boulders and scoured downstream. Because the
31 Q_{50} flow was not able to re-work the channel by disrupting grain-interlocking from preceding
32 lower flows, transporting boulders, or forming channel-spanning boulders, the channel-forming
33 discharge is larger than the Q_{50}. These results have implications for restoration of gravel
34 spawning beds in northern Fennoscandia and highlight the importance of large grains in
35 understanding channel morphodynamics.

36

37

38

39

40

41

42

43

44

45

46

47

48

Plain language summary

Many streams in northern Scandinavia and Finland contain abundant boulders that were originally deposited by glaciers (>10,000 year ago). However, most of these so-called 'semi-alluvial' streams were heavily altered during the timber-floating era. In order to understand how these streams should look naturally and change over time, experiments were conducted mimicking this stream type. An experimental stream was built in a flume (8 x 1.1 m) with down-scaled sediment sizes matching that of streams in northern Sweden. With two different slopes (2% and 5%), four flows were run to mimic flows ranging from the annual high flow to the 50-year flood. Because lakes are common along these streams, high recurrence-interval flows (that occur rarely) are not as large as in mountain streams. Therefore, boulders barely moved even with the 50-year flood at the 2% slope and only rolled slightly at the 5% slope (due to downstream scour). During 10-year and 50-year floods, finer sediment deposited upstream and eroded downstream of boulders. Contrary to mountain streams with coarse boulders, a flow much greater than the 50-year flood is necessary to re-work the channel bed. These results have implications for stream restoration, including providing habitat and spawning gravel for trout and salmon.

1 Introduction

1.1 Semi-alluvial channels

Semi-alluvial channels have commonly been described as those where a cohesive boundary, most commonly bedrock or cohesive clays, either composes the channel banks, thus confining the channel from lateral migration, or the channel bed, thus constraining the channel from degrading (Coulombe-Pontbriand & LaPointe, 2004; Meshkova et al., 2012; Turowski, 2012). Another type of semi-alluvial channel exists where the channel contains abundant cohesive or coarse sediment, which are fixed immobile points in the channel and have not been deposited by alluvial processes (Pike et al., 2018). This potentially immobile sediment has been referred to either as lag or legacy deposits in cases where mass wasting has caused an input of coarser material (e.g., Brummer & Montgomery, 2003), where lahar deposits below the channel inhibits incision (Reid et al., 2013), or where a previous geomorphic process regime, such as glaciation, has deposited sediment that is currently immobile within the current fluvial hydrological regime (Gran et al., 2013; Polvi et al., 2014). Semi-alluvial channels with glacially-derived sediment from depositional landscapes formed by continental ice sheets may contain non-alluvial patches that are (1) easily eroded and form alluvial deposits, (2) cohesive fine-grained material that only responds to extreme high flows (Pike et al. 2018), or (3) coarse-grained cobbles and boulders (Ashmore & Church, 2001; Polvi et al., 2014). Such semi-alluvial channels with till beds, containing either cohesive sediment or sand, gravel and large boulder clasts, are common on Canada's Southern Shield and Southern Boreal Shield (Ashmore & Church, 2001) and in northern Fennoscandia (Polvi et al., 2014). In such systems, where all sediment was not deposited by fluvial processes and is potentially unable to be reworked even by high recurrence-interval high flows, it is unknown whether the mobile sediment self-organizes into predictable bedforms or whether predictable patterns of sediment clusters and scour form.

90   In northern Fennoscandia, boulder-bed semi-alluvial channels are common (Polvi et al.
91 2014; Rosenfeld et al., 2011), as the landscape has been shaped by several episodes of
92 continental glaciation. Glacially drifted till is the most common deposit in Fennoscandia,
93 forming various landforms in the form of ribbed and Rogen moraines, drumlins, eskers, and
94 erratics (Seppälä, 2005). Semi-alluvial channels are found in tributary catchments to large rivers
95 that flow from the mountains to the Baltic Sea in areas with mapped fluvio-glacial sediment in
96 longitudinal swaths (Geological Survey of Sweden surficial geology maps, 1:25,000- 1:100,000).
97 The tributaries are divided into three main process domains, which are spatially separate zones
98 with distinct suites of geomorphic process (*sensu* Montgomery, 1999): lakes, slow-flowing
99 reaches in peat or fine sediment (S_0: <0.01 m/m), and semi-alluvial rapids (S_0: 0.005-0.07 m/m)
100 (Figure 1). Similar systems with abundant mainstem lakes and 'steeps' and 'flats' have been
101 described by Snyder et al. (2008, 2012) in a similarly glaciated landscape in Maine, USA.
102 Putting semi-alluvial rapids within the context of their stream network organization of process
103 domains is necessary to understand reach-scale sediment processes. Mainstem lakes buffer
104 sediment and water fluxes, which reduce the available fine sediment input from upstream reaches
105 (Snyder et al., 2012) and may preclude very high flows (Leach & Laudon, 2019). Thus, to
106 summarize, a process-based understanding of morphodynamics in semi-alluvial rapids in
107 northern Fennoscandia is hampered by two geomorphic factors: (1) streams are semi-alluvial, in
108 that they contain coarse glacial lag sediment (till from moraines and subglacial tunnels) and (2)
109 numerous mainstem lakes buffer sediment and water fluxes.

110   Furthermore, natural reference sites are lacking due to extensive timber-floating (mid
111 1800s to ~1980) that caused widespread channelization and clearing of rapids, so stream
112 restoration schemes cannot rely on copying existing reference sites. In these rapids, some of
113 which were unimpacted and others of which were channelized and later restored, no clear pool-
114 riffle or step-pool bedforms have been observed in the field (*personal observation*), and cascade
115 bedforms have been observed at slopes where plane bed, alternate bar, or step-pools should form
116 in alluvial channels (S_0: ~0.04-0.07 m/m, *sensu* Montgomery & Buffington, 1997; Palucis &
117 Lamb, 2017). Due to the widespread nature of timber-floating, which necessitated channelization
118 and clearing of coarse boulders (through manual clearing, the use of dynamite and bulldozers),
119 virtually no unimpacted reference reaches exist (Nilsson et al., 2005). Most of those that were
120 unimpacted by channelization—though were still impacted by clearing of instream wood,
121 harvesting of old-growth riparian trees, and flow diversion—are steeper than those that have
122 been restored (Polvi et al., 2014). In the past decade, several stream restoration projects have
123 attempted to restore these semi-alluvial rapids because of the low salmonid populations and
124 negative effects on biodiversity (Gardeström et al., 2013); however, very little research or
125 knowledge on the processes governing sediment transport and organization in these streams are
126 available (except Rosenfeld et al., 2011).

127
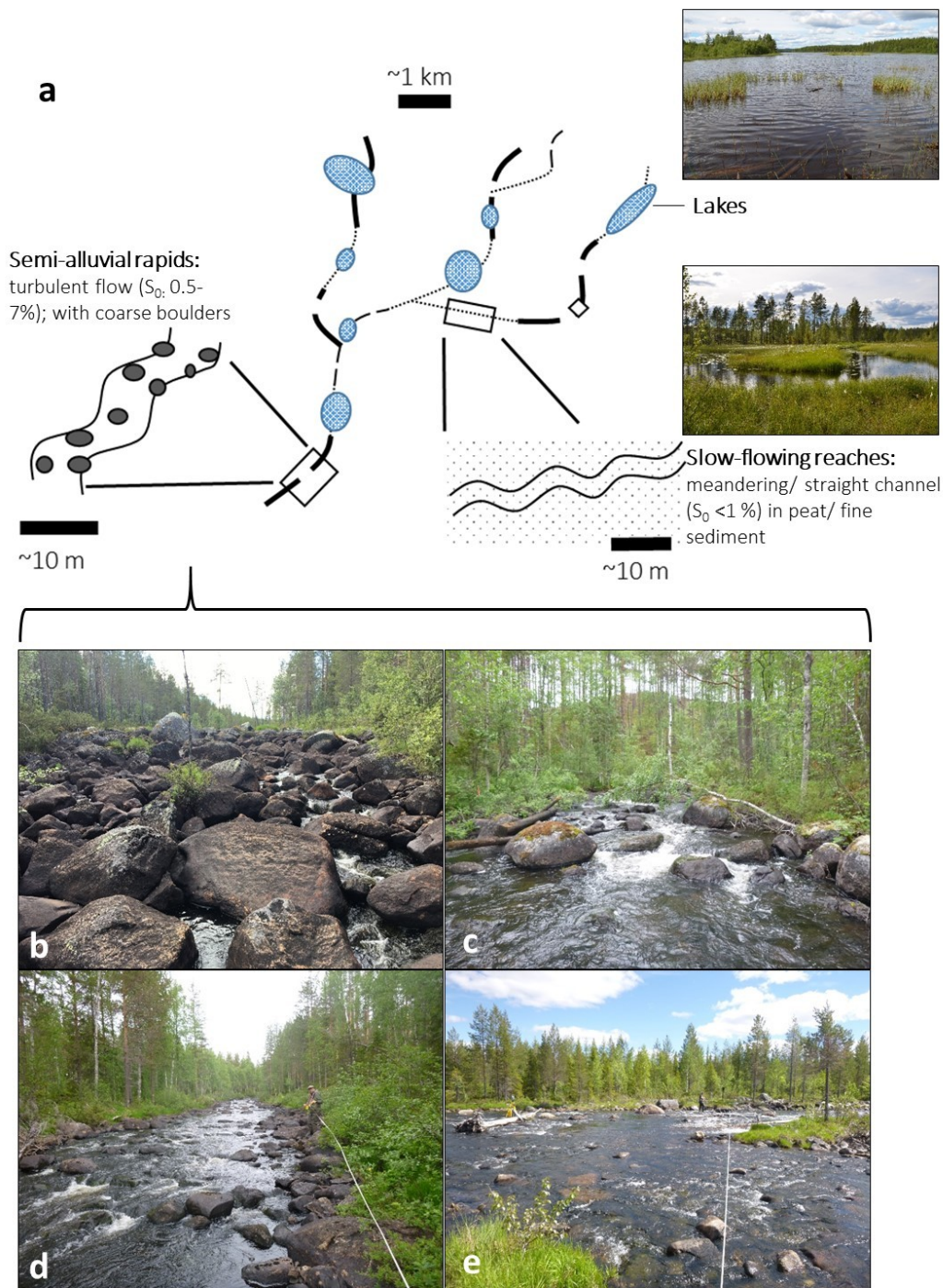
128
Figure 1. (a) Schematic of stream networks in tributary streams in northern Fennoscandia.
Streams are segmented into three process domains: semi-alluvial rapids, slow-flowing reaches
and lakes, with four examples of prototype reaches of semi-alluvial rapids (b-e). Photos b & c are
of unimpacted reaches with channel bed slopes of 0.05 and 0.04 m/m, respectively; photos d & e
are of restored reaches with channel bed slopes of 0.03 and 0.02 m/m, respectively. In photos b-
d, the flow direction is out of the picture, and in photo e, the flow direction is from right to left.

135   1.2 Background

136   The channel geometry and bedforms found in semi-alluvial channels are not easily
137   predicted based on slope or bankfull discharge. Forms and processes of alluvial streams, on the
138   other hand, have been well-studied, allowing prediction of sediment transport, channel geometry,
139   and bedforms (Church, 2006; Faustini et al., 2009). For example, regionally-derived downstream
140   hydraulic geometry equations can be used to predict channel width, depth, and velocity based on
141   relationships with bankfull discharge or drainage area, because these channel geometry
142   parameters reflect the stream's equilibrium conditions (Church, 2006; Leopold & Maddock,
143   1953). Even in steep, coarse-bed channels, channel bed slope can predict bedform morphology
144   (e.g., step-pools, plane bed or pool-riffle), which may reflect a balance between sediment supply
145   and transport capacity (Montgomery & Buffington, 1997) or other processes co-varying with
146   slope (Palucis & Lamb 2017). In addition, the formation of and the controlling mechanisms of
147   sediment sorting in step-pools and pool-riffles have been examined, showing that these bedforms
148   reflect a self-organization phenomenon that form in order to dissipate energy (Chin & Wohl,
149   2005), and that sediment is preferentially stored in and mobilized from pools (e.g, Sear, 1996).

150   Some insight into semi-alluvial channels with coarse glacial sediment are available from
151   experiments based on mountain streams with boulder-bed channels. In general, the effects of
152   boulders on local sediment transport are poorly understood due to local feedbacks between
153   hydraulics and bed response (Monsalve & Yager, 2017; Nitsche et al., 2012; Yager et al., 2007).
154   Finer sediment patches commonly form on the lee side of protruding clasts due to flow
155   separation (Thompson, 2008), which in turn alter local roughness, affecting hydraulics and thus
156   sediment transport around boulders (Laronne et al., 2001). However, in boulder-bed channels
157   with low relative submergence (h/D <3.5, where h is the flow depth and D is the boulder
158   diameter; Papanicolaou & Kramer 2005), experimental studies have documented deposition of
159   fine to medium-sized sediment directly upstream of boulders (Monsalve & Yager, 2017;
160   Papanicolaou et al., 2018). Monsalve and Yager (2017) explained the formation of upstream
161   patches as a consequence of negative shear stress divergence upstream of boulders and an
162   increase in dimensionless shear stress downstream of boulders in channels with low relative
163   submergence (RS); however, this study used a simplified system with regularly spaced equi-
164   sized hemispheres, spaced so that wakes between consecutive boulders did not interfere with one
165   another. Furthermore, the presence of protruding boulders can absorb a significant amount of
166   shear stress so that the available shear stress for entrainment and transport of mobile sediment
167   decreases, leading to potential overestimation of sediment transport (Papanicolaou et al., 2012;
168   Yager et al., 2007, 2012).

169   On a larger spatial and longer temporal scale than sediment deposition dynamics,
170   processes that drive bedform development and steer which flow is channel-forming may differ
171   for semi-alluvial and alluvial channels. In steep, coarse- (gravel, cobble, and boulder) bed
172   alluvial channels, bed slope can predict either a unique bedform or multiple stable states (Palucis
173   & Lamb, 2017). For example, according to Montgomery & Buffington (1997), step-pool
174   channels commonly have slopes ranging from 0.03 to 0.065 m/m; however, further studies have
175   shown that only individual steps form at slopes around 0.04 m/m and continuous steps require
176   slopes exceeding 0.07 m/m (Church & Zimmerman, 2007). At lower slopes, stone lines or
177   transverse ribs form out of cobbles and boulders, without channel-spanning pools; however,
178   these are commonly submerged even at moderate flows (Church & Zimmerman, 2007). In terms

179 of the role of sediment, the formation of step-pools is a combination of the random location of
180 keystones, at which other large grains come to rest (Curran & Wilcock, 2005; Lee & Ferguson
181 2002; Zimmerman & Church, 2001), and hydraulics, where step-pools form under antidune
182 crests at high discharges so that scour occurs on the falling limb creating a pool between coarser
183 deposits (Grant, 1997; Lenzi, 2001; Whittaker & Jaeggi, 1982). Based on these step-forming
184 hypotheses, the limiting factor for forming steps in boulder-bed semi-alluvial channels will not
185 be keystone clasts but rather the ability for additional large grains to deposit upstream of
186 keystones and for sufficient scour to take place downstream of keystones.

187   Furthermore, regardless of whether step-pools or any other bedform or regular sediment
188 cluster can form, there is the question of which flow creates and then maintains the current
189 channel configuration, in terms of bedforms and boulder configuration. It is debated whether the
190 effective discharge, defined as the flow that transports the most sediment over time, is also the
191 discharge that determines the channel morphology (Andrews, 1980; Emmett & Wolman, 2001;
192 Lenzi et al., 2006a; Torizzo & Pitlick, 2004). Although effective discharge originally referred to
193 transport of suspended sediment (Wolman & Miller, 1960), this concept has also been applied to
194 bedload transport (e.g., Lenzi et al., 2006a; Torizzo & Pitlick, 2004). In many alluvial channels,
195 the bankfull flow, with a 1.5-2 year recurrence interval, does the most geomorphic work and is
196 the flow to which the channel has adjusted (Andrews, 1980; Phillips and Jerolmack, 2016).
197 However, depending on the system, the effective discharge for bedload may be discordant with
198 the channel-forming flow (e.g., Downs et al., 2016) and may instead be a channel-maintaining
199 discharge, while a more infrequent flow shapes the channel (Lenzi et al., 2006a). For example, in
200 alluvial, snowmelt-dominated Rocky Mountain streams, the effective discharge reflects rare
201 events (e.g., Q_{50}) in plane-bed channels, whereas the effective discharge is nearer the Q_{bf} flow in
202 step-pool channels (Bunte et al., 2014); however, the channel-forming discharge for step-pool
203 channels often reflects a higher recurrence-interval flow (Lenzi et al., 2006b). Similarly, in a
204 study in formerly glaciated mountain streams of British Columbia, the effective discharge was
205 overall very frequent but was also highly variable, depending on the threshold for gravel-sized
206 sediment transport (Hassan et al., 2014). Hassan et al. (2014) distinguished three stream types in
207 British Columbia based on whether there was mobile or immobile gravel or whether sand was
208 transported over gravel. Channels with mobile gravel exceeded the effective discharge multiple
209 days per year, channels with immobile gravel had very low-frequency, high-magnitude effective
210 discharges, and those with mobile sand but immobile gravel showed a bimodal effective
211 discharge. Therefore, there may be a low effective discharge that does not, however, equal the
212 channel-forming discharge. In addition, the presence of large boulders and thus low relative
213 submergence increases the flow resistance (Bathurst, 2002). For example, the most accurate
214 equations to predict the grain component of flow resistance require the D_{84} in addition to D_{50}
215 (Bray, 1979; David et al., 2011; Hey, 1979). Thus the available shear stress to mobilize sediment
216 is reduced (Yager et al. 2007). Therefore the potential of flows to transport sediment decreases
217 which should increase the channel-maintaining or channel-forming discharge.
218
219   Predictions of potential sediment transport and channel re-working depend not only on
220 shear stresses associated with different flow magnitudes, but also on the flow history since a
221 channel-reworking flow (Masteller et al., 2019). During low-magnitude flows, sediment is
222 locally rearranged and particle interlocking increases, thus increasing the critical shear stress for
223 particle movement (Reid et al., 1985). However, during high-magnitude flow events, particle
224 interlocking is disrupted and the critical shear stress decreases, allowing for much higher

225 transport rates (Turowski et al., 2009; Masteller et al., 2019). Thus, the probability of sediment
226 transport depends on prior flows, including the time since a high-magnitude, sediment
227 transporting flow (Masteller et al., 2019; Yager et al., 2012), which may thus account for a large
228 portion of the variability in dimensionless shear stress values (Johnson, 2016). Therefore, when
229 determining whether a flow is capable of re-working the channel, the probability of a high flow
230 reworking the channel decreases if a channel has experienced previous low or medium flows. So,
231 a more conservative estimate (avoiding underestimations) of a channel-forming flow should be
232 based on a channel where the sediment has been locally rearranged with particle interlocking
233 thus exhibiting a critical shear stress on the higher end within the range of variability.

234 1.3   Objectives

235   In order to gain insight of the morphodynamics of semi-alluvial boulder-bed channels , a
236 flume study was designed and carried out to mimic conditions in previously field-studied semi-
237 alluvial rapids in northern Sweden (Polvi et al., 2014). The objective of this study was to model
238 the potential evolution of bedforms or self-organization of sediment in semi-alluvial channels
239 with coarse glacial legacy sediment using a range of flows (annual high-flow to 50-year flood) in
240 a flume at two different slopes (0.02 and 0.05 m/m). I aimed to answer the following questions:
241 (1) given a history of potentially stabilizing, low flows, can we determine the potential range of
242 channel-forming discharges? Specifically, is a large-magnitude flow (e.g., Q_{50}) capable of
243 reworking the channel, transporting boulders and creating bedforms? Here, I define channel-
244 forming discharge as a flow that can transport boulders and re-organize potential bedforms or
245 sediment clusters. This question is addressed through observations of potential boulder transport
246 and by calculating the event-based and cumulative geomorphic work by each flow given a
247 specific order of flows. Whether or not the geomorphic work during the Q_{50} flow exceeds that of
248 the Q_1 or Q_2 flows will determine whether the higher flow is capable of re-organizing the bed. (2)
249 Do patterns of sediment erosion and deposition form around large, potentially immobile
250 boulders? This builds on the literature of boulder-bed channels in low relative submergence
251 regime systems. These results will provide management recommendations on how to best
252 restore these semi-alluvial channels in a self-sustaining manner.

253 1.4 Prototype description

254   The flume study modeled semi-alluvial boulder-bed stream channels found in tributaries
255 to the free-flowing Vindel River, which with a drainage area of ~12,500 km^2 is the largest
256 tributary to the Ume River that flows into the Baltic Sea from the Scandes Mountains at the
257 Swedish-Norwegian border. From the mid-1800s to the 1970s, the stream networks were used as
258 a transport system for timber from the inland forests to the coastal sawmills, and thus nearly all
259 semi-alluvial channels were channelized. Channelization involved manual clearing of coarse
260 sediment, closing off side channels, building levees with coarse sediment (cobbles and boulders),
261 and later using bulldozers to clear the middle of the channel. Restoration started in the 1990s
262 with 'basic restoration' that entailed returning coarse sediment from levees to the main channel
263 and opening up some side channels (Gardeström et al., 2013). In 2010, 'enhanced restoration'
264 commenced that involved significantly widening the channel and obtaining large boulders (>1
265 m) from the surrounding forest that were placed into the channel in addition to the cobbles and
266 boulders that remained along the channel edge (Gardeström et al., 2013). Although virtually all

267 semi-alluvial rapids were channelized, some unimpacted reaches remain but most of them are
268 steeper than those that were channelized and subsequently restored (Polvi et al., 2014).

269   In this study, two prototype channels were used, representing enhanced restored reaches
270 (note: enhanced restored reaches are referred to as 'demo restored' reaches in Polvi et al., 2014)
271 and unimpacted reaches (Figure 1). Channel geometry and sediment distribution parameters were
272 obtained from four unimpacted and five enhanced restored stream reaches described in more
273 detail in Polvi et al. (2014). The average channel bed slope of the enhanced restored reaches was
274 ~0.02 m/m (range: 0.015-0.037 m/m), whereas unimpacted reaches had an average slope of
275 ~0.05 m/m (range: 0.029-0.074 m/m). The remainder of the channel geometry parameters,
276 including width, depth and sediment distribution, was similar between the two groups of reaches
277 (Polvi et al., 2014); channel widths range from 7-20 m and average bankfull depths are 0.5-1 m.
278 The catchments, which vary in drainage area from 9-151 km^2, consist of an average of 2.53%
279 lakes (0.04-6.65%), all of which are connected to the stream network, and an average of 21%
280 wetlands (6.00-52.40%) (SMHI, 2015). Sediment distributions were obtained from 300-particle
281 pebble counts of the nine reaches. The average median grain size was 245 mm (range: 130-400
282 mm), average 84th percentile sediment size was 624 mm, and average maximum sediment size
283 was 1670 mm (range: 1400-5000 mm). There was less than 10% sand, and examination of the
284 sub-surface sediment did not reveal higher percentages of sand; i.e., there is not substantial
285 armoring that shields a buried sand layer. This is further supported by the low rates of
286 weathering and sediment production in the region, as suggested by global-scale sediment yield
287 maps (Lvovich et al., 1991; Walling & Webb, 1983) and quantification of annual sediment flux
288 in a nearby catchment of only ~55 t/km^2 (Polvi et al., 2020), which is due to the relatively low
289 relief, crystalline bedrock (and till), and cold climate. Because of the segmented channel
290 network, where mainstem lakes are abundant, there is probably very little sediment transport of
291 fine grain sizes from upstream high-gradient reaches (Arp et al., 2007).

292   The flow regime in northern Sweden is dominated by snowmelt-runoff high flows in the
293 spring/early summer. The average annual precipitation is 600 mm, of which 40% falls as snow
294 (SMHI, 2017). The numerous mainstem lakes serve to buffer high flows, therefore low-
295 recurrence interval floods do not substantially increase in magnitude compared to higher-
296 recurrence interval floods, as seen in ratios of recurrence interval flows (Bergstrand et al., 2014).
297 For example, the Q_{50} flow is less than twice that of the Q_2 flow (Q_{50}/Q_2 = 1.8), and even the
298 predicted Q_{100} and Q_{500} flows are only 1.12 and 1.4 times that of the Q_{50} flow, respectively
299 (Figure S1). Ice forms in most of these channels during winter, as either surface or anchor ice
300 and flooding due to ice cover and ice jamming is also common (Lind et al., 2016). Although
301 there are few studies studying the role of ice formation and break-up on sediment transport,
302 Lotsari et al. (2015) found that boulders (up to 2 m in diameter) embedded in ice can be
303 transported downstream during ice break-up. Polvi et al. (2020) quantified the amount of
304 sediment transport under ice and during ice break-up as ~5% of annual sediment yield. However,
305 the potential effect of ice varies within a catchment, as no anchor ice forms and little surface ice
306 forms in reaches close to an upstream lake (Lind et al., 2016).

307

2 Methods

2.1 Flume setup

A mobile-bed physical model of the semi-alluvial prototype streams in northern Sweden was set up in an 8-m long, 1.1-m wide fixed-bed flume at the Colorado State University Engineering Research Center in Fort Collins, Colorado, USA (Figure 2). Using a geometric (y_r and z_r) scaling factor of 8, the initial sediment distribution was scaled-down to be analogous to that in the semi-alluvial prototype streams, and because the flume D_{10} was 4 mm and D_{min} was 0.14 mm, all sizes were sand-sized or above so there were no issues with cohesiveness (Table 1). No sediment feed was provided from upstream, creating clear water conditions, and this is consistent with the prototype field conditions with very low levels of suspended sediment or annual sediment flux (Polvi et al., 2020) and little sediment input from the hillslopes or upstream reaches. Two flume setups were used with initial bed slopes of 0.02 and 0.05 m/m, respectively. Before the flows were run, the grain size distribution was thoroughly mixed in the flume, and checks were made to ensure equal sediment depth and the desired slope throughout the flume length. For each slope, four runs were conducted with flows analogous to the summer high (Q_1), the 2-year (Q_2), 10-year (Q_{10}), and 50-year (Q_{50}) flows in the prototype streams. The flows were run in a sequence from the lowest to highest flow, with initial bed conditions for each flow equal to that of the final conditions of the preceding flow. The summer high flow (Q_1) was not based on a bankfull flow that filled the banks in the flume channel, but rather based on field conditions in the prototype channels. Flow measurements were taken in the field at the summer high flow, which was close to or just below the geomorphically-defined bankfull flow (Gardeström J.*, unpublished data*) (see Section 2.2. for a full description of flows). Each flow was run for 60 minutes, which surpassed the time necessary until equilibrium conditions were met, as defined by minimal to no visible sediment transport or transport out of the reach. As no boulder ($>D_{84}$) movement was detected (other than slight rotation, as described in Results) during any flow, equilibrium conditions were only based on transport of the fine sediment fraction. After each flow, the bed topography and channel geometry were measured (described below in Section 2.3) before running the next higher flow. After the flume's slope was altered from 0.02 to 0.05 m/m, sediment lost from the previous slope setup was returned and all sediment was manually mixed with shovels, so that the initial conditions for both slopes were approximately the same, with a plane bed and well-mixed sediment sizes. This experimental setup means that initial conditions were different for the two slopes and for each flow. However, due to the wide sediment size distribution, it would be nearly impossible to replicate initial conditions for each flow and slope. Therefore, the results should not be used to compare processes between slopes but to be used as two case studies of boulder-bed semi-alluvial reaches. The bed degraded slightly during each subsequent flow, as seen through an increase in slope: for the 2% slope setup, the centerline slope started at 0.022 m/m and changed to 0.0211, 0.0223, 0.0226, and 0.0222 m/m with each consecutively higher flow; for the 5% slope setup, the centerline slope started at 0.0532 m/m and changed to 0.0538, 0.0538, 0.0549, and 0.0545 with each consecutively higher flow. However, this reach-scale degradation is fairly minor in terms of changing initial conditions for each flow, and the centerline slope was controlled more by local sediment re-arrangement rather than reach-scale degradation. With this setup, channel width could not adjust; however, due to the coarse sediment sizes, it is assumed that adjustment of the channel would occur via downstream sediment transport rather than streambank erosion and lateral migration.

352

353

354
355 **Figure 2.** Photos of each flume run at two slope setups with four different flow magnitudes.
356 Pictures a-d were taken at the 2% slope setup, and pictures e-h were taken at the 5% slope setup.
357 Photos a & e were taken at Q_1 (0.006 m^3/s); photos b & f at Q_2 (0.017 m^3/s); photos c & g at Q_{10}
358 (0.025 m^3/s); and photos d & h at Q_{50} (0.031 m^3/s).

359

360

361

362   **Table 1.** Prototype Reach Characteristics and Corresponding Flume Specifications

	Prototype reach characteristics	Flume specifications
Bed Slope	Restored channels: 0.8-3.7%	Setup 1: 2%
	Unimpacted channels: 2.9-7.4%	Setup 2: 5%
Width	8.8 m	1.1 m
Length	64.0 m	8.0 m
Sediment Input	Crystalline rocks, low levels of weathering, and abundant lakes that buffer sediment = low levels of suspended sediment	Clear water (no sediment feed)
Initial Conditions	Rapids form in poorly sorted till within moraines and eskers	Unsorted sediment mix, with plane bed morphology
Sediment size distribution		
D_{16}	56 mm	7 mm
D_{50}	248 mm	31 mm
D_{84}	624 mm	78 mm
D_{max}	1672 mm	209 mm
Flows/unit discharges		
Q_1	1.0 m³/s / 0. 125 m²/s	0.006 m³/s / 0.005 m²/s
Q_2	3.1 m³/s / 0. 062 m²/s	0.017 m³/s / 0.015 m²/s
Q_{10}	4.6 m³/s / 0.577 m²/s	0.025 m³/s / 0.023 m²/s
Q_{50}	5.6 m³/s / 0.705 m²/s	0.031 m³/s/ 0.028 m²/s

363

364   2.2 Flume flows

365   For each of the four unimpacted and five enhanced restored stream reaches studied in
366   Polvi et al. (2014), the various flow magnitudes that represent the Q_2, Q_{10} and Q_{50} flows were
367   derived from a hydrological model, S-HYPE, developed by the Swedish Meteorological and
368   Hydrological Institute (Lindström et al., 2010; SMHI, 2015). The model (HYdrological
369   Predictions for the Environment) makes sub-basin scale hydrological calculations based on the
370   basin-characteristics of surficial geology, landuse, altitude, lake depth, and stream length, and
371   temporal inputs of sub-basin mean daily temperature and precipitation (Lindström et al., 2010).
372   The average of each of these flows for the nine reaches were used to calculate the desired
373   discharge for the flume runs. The Q_1 flow magnitude was based on high flow field-measurements
374   of enhanced restored streams (Gardeström J., *personal communication*); although this may not
375   equate to a flume channel-filling flow, it is analogous to the flow magnitude experienced by the
376   prototype channel most years directly after the snowmelt-induced spring flood. The experimental
377   flows were scaled down by a factor of 181.02 according to equation (1) following Froude
378   number similitude over fixed beds (Julien, 2002).

379     $$Q_r = y_r z_r^{\frac{3}{2}}$$ (1)

380 where, Q_r is the discharge scaling factor, and y_r and z_r are the lateral and vertical scaling factors,
381 respectively, which were both set to 8.

382 Although the objective of this study was to model temporal evolution of the bed and potential
383 bedforms, scale effects used for mobile bed Froude models was not deemed to play a significant
384 role. Because the main objective of scaling the discharge was to obtain relative changes in flow
385 that correspond to different recurrence intervals in the field, exact correspondence to a specific
386 flow was not necessary. Also in Froude scaling, non-dimensional shear stress scales directly,
387 thus entrainment of model particles will be equal to that in the field. For each flume setup, a
388 low-flow discharge was run first to provide saturated conditions prior to the experimental runs.
389 Discharge was measured in a closed pipe prior to the inflow in the flume using a Badger-meter
390 M2000 flow meter. Before entering the flume, the inflow was allowed to mix in a 'crash box' for
391 ~0.5 m to dampen turbulence before entering the flume. The top 0.5 m of the flume was lined
392 with very coarse sediment so that preferential scour and sediment entrainment did not occur
393 where the water first entered the flume over a lip. Morphologic measurements started
394 downstream of the coarse sediment buffer zone. Likewise, at the downstream end of the flume,
395 sediment was preferentially transported as a headcut formed. However, the morphologic analyses
396 were cut off where this effect was seen.

397 2.3 Morphologic & hydraulic data acquisition and analyses

398   Structure-from-motion photogrammetry (SfM) was used to create digital elevation
399 models (DEMs) of bed topography (Westoby et al., 2012). SfM-created DEMs were constructed
400 before all runs at each slope setup and after each run, with progressively higher flows. For each
401 flume setup with different slopes, a terrestrial LiDAR scan (TLS) was used to determine a
402 coordinate system and be able to georeference the SfM scans, based on targets affixed to the
403 flume walls. The TLS scans provided exact xyz coordinates of the targets, which were used to
404 georeference the SfM-based DEMs. A Canon EOS Rebel T3i DSLR camera with a fixed, non-
405 zoom lens (Canon EF-S 24 mm prime lens), which minimizes edge distortion of photos, was
406 mounted to a movable cart on rails ~30 cm above the flume bed. Photos were taken ~20 cm apart
407 looking upstream and downstream at an oblique 45° angle. This flume setup and sediment
408 distribution was included in a study comparing results from SfM and TLS scans, which found
409 that SfM can produce topographic point clouds with comparable quality and greater point
410 densities to TLS (Morgan et al., 2017), thus verifying the validity of the SfM scans in this study.
411 The images were processed using AgiSoft PhotoScan Professional (Agisoft LLC, 2014) to obtain
412 topographical point clouds.

413   The topographical point clouds were imported into ArcMap 10.5.1 (ESRI, 2017) and
414 rasters were created with a grid size of 5 mm to create digital elevation models (DEMs) of the
415 topography for the initial conditions at each slope setup and after each flow with a precision of 2
416 mm (Polvi, 2020; Figure 3). In areas with missing data, the neighboring points were iteratively
417 averaged to interpolate elevations for pixels. The flume study area was clipped to 7.0 m and 6.3
418 m in length for the 2% and 5% slope setups, respectively, to remove the upstream turbulent
419 section containing much coarser sediment and a headcutting section at the downstream portion of
420 the flume. To analyze differences in aggradation versus degradation after each run, the DEMs
421 were subtracted from one another to create DEMs of difference (DoDs) (Wheaton et al., 2010);
422 DoDs were created comparing each flow to the initial conditions and after each successive flow.

423   In addition, all large clasts, defined as sediment clasts >D_{84} (~80 mm in diameter), were digitized
424   (Polvi 2020), and the spatial distribution of aggradation and degradation in relation to the large
425   clasts were analyzed by creating buffers equal to half the diameter of the respective clasts. Each
426   buffer was then split into an upstream and downstream half, and the mean elevation change in
427   each upstream and downstream buffer was calculated using zonal statistics within ArcGIS. One-
428   sample t-tests were used to determine whether the mean elevation change in all of the upstream
429   and downstream buffers after a given flow, compared to the previous flow and compared to the
430   pre-flow conditions, were significantly different from 0. Two-sample t-tests were used to
431   determine whether the mean elevation change differed between the upstream and downstream
432   buffers for a given flow compared to the previous flow and compared to the initial conditions.
433   Although some downstream buffers were close to or slightly overlapped with an upstream buffer
434   for another clast, or vice versa, the effect of other large clasts in the vicinity of a buffer may
435   contribute to variation in the mean values but should not affect the overall mean values. All
436   statistical analyses were performed using the statistical software 'R' (RStudio Team, 2016).

437   The total geomorphic work done by each flow was calculated as the sum of the volume of
438   aggradation and degradation in the entire flume area, which is different than the standard method
439   of using transport rates and assumes that large channel changes implies relatively high transport
440   rates. Because the flows were run in order from lowest to highest for each slope setup, the
441   geomorphic work for the higher flows may be underestimated due to interlocking of grains
442   during lower flows (e.g., Masteller et al., 2019); therefore, the geomorphic work for each flow is
443   also reported as the cumulative combined aggradation and degradation of that flow in addition to
444   all prior flows. To determine how much the sediment was reworked after each flow, the percent
445   of the flume area that experienced erosion or deposition was calculated by determining how
446   many pixels (5 mm x 5 mm) in DoDs experienced >0.01 m or < -0.01 m of elevation change and
447   by transforming this to a percent of the entire bed. Thresholding of the DoDs was only done for
448   visualization purposes (Figures 4a, S2, S3) and for calculation of the area affected by erosion or
449   deposition (>0.01 m of elevation change). For the volume analysis of erosion/deposition,
450   potential errors would contribute to negligible or small volumes compared to actual change. For
451   the D_{84} buffer analysis, random errors should cancel each other out (positive and negative
452   change) in calculation of mean elevation change. DEMs were detrended to visualize topography
453   throughout the entire reach (Figure 3). Using the detrended DEMs, topographical roughness was
454   calculated as the standard deviation of elevation values.

455   Because the main objective of this flume experiment was to analyze changes in
456   morphology, detailed hydraulic measurements were not made. However, flow depths were
457   recorded longitudinally spaced throughout the channel and at three lateral locations during each
458   flow. Missing flow depth data from the first two flows at the 2% slope setup were estimated
459   using time-lapse photos during the runs and DEMs by measuring flow depths based on the water
460   surface elevation. Reach-scale averages of flow depth were used to calculate the reach-averaged
461   shear stress (Equation 2), relative submergence, and Froude number. Because the critical shear
462   stress required to entrain larger than D_{50} grain sizes does not increase linearly, but is lower due to
463   protrusion effects (e.g., Ashworth & Ferguson, 1989), only the dimensionless shear stresses (τ^*)
464   on D_{50}-sized sediment for each flow and slope were calculated using Shield's equation
465   (Equation 3). These values were then compared with critical dimensionless shear stress (τ_c^*)
466   values of 0.1, which may be more accurate for steep streams with low relative submergence

467 (Lenzi et al., 2006b), and those calculated based on Lamb et al.'s (2008) slope-dependent
468 regression (Equation 4).

469 $\tau = \rho_w g h S$ (2)

470 where, τ is the reach-scale shear stress (N/m^2), ρ_w is the density of water (1000 kg/m^3), g is
471 acceleration due to gravity (9.81 m/s^2), h is the average flow depth, and S is the reach-averaged
472 bed slope.

473 $\tau* \lnot \dfrac{\tau}{\left(\rho_s - \rho_w\right) g D_{50}}$ (3)

474 where, $\tau*$ is the dimensionless shear stress, D_{50} is the median grain size (m), τ is the reach-scale
475 shear stress (N/m^2), ρ_s is the density of sediment (2650 kg/m^3), ρ_w is the density of water (1000
476 kg/m^3), and g is acceleration due to gravity (9.81 m/s^2).

477 $\tau* \lnot_c = 0.15 S^{0.25} \lnot$ (4)

478 where, $\tau*_c$ is the critical dimensionless shear stress and S is the bed slope (m/m) (Lamb et al.,
479 2008).

480
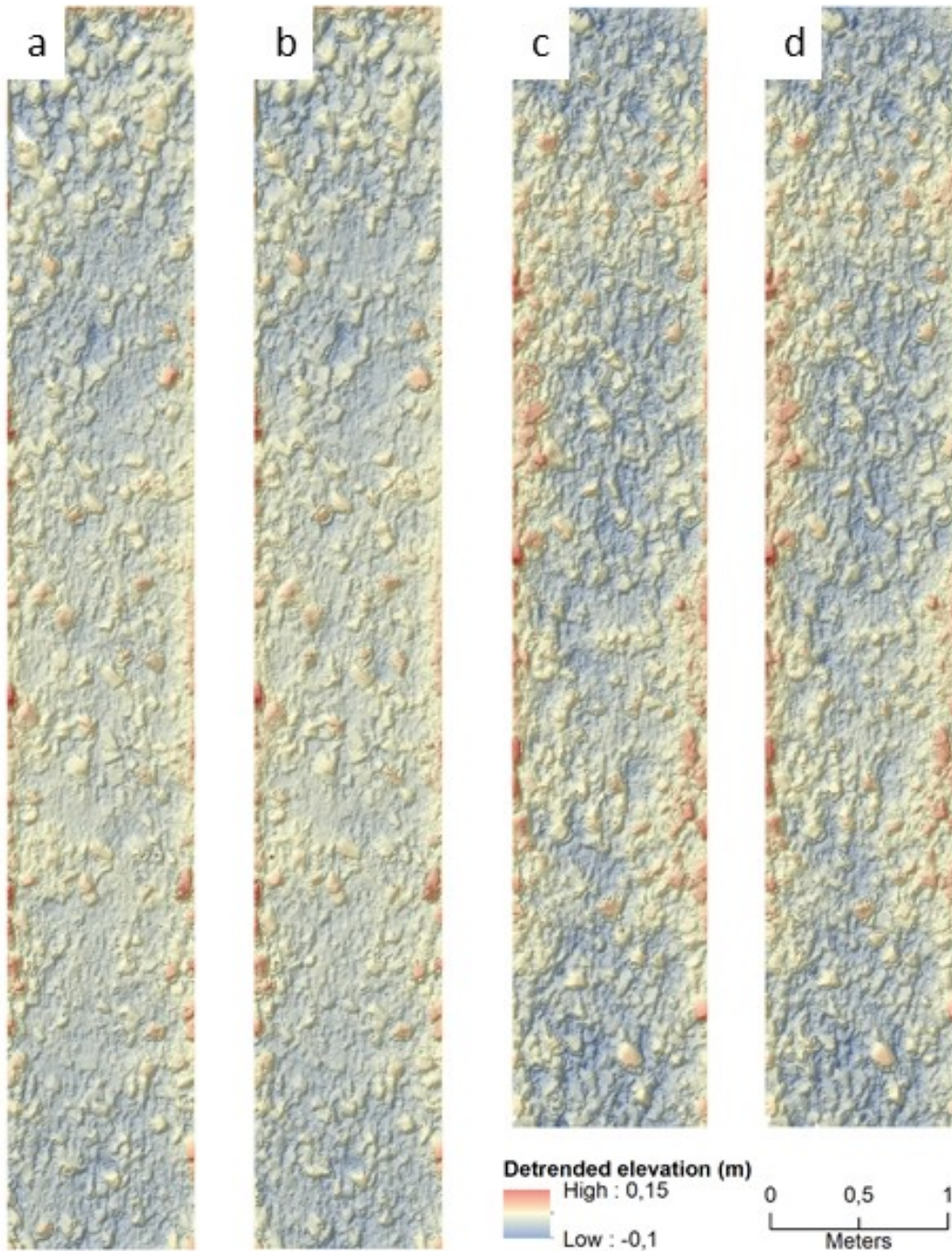
Figure 3. Detrended digital elevation models based on structure-from-motion photogrammetry at the 2% slope setup (a & b) and 5% slope setup (c & d), showing initial conditions (a & c) and channel bed topography after the Q_{50} flow (b & d). Color scales show relative detrended elevations in meters. Distance scale bar applies to all DEMs. Note that the analyzed flume area was slightly shorter with the 5% slope setup due to the larger affected area by headcutting.

487 **3 Results**

488 3.1 General visual observations

489   At both slope setups, the large clasts ($>D_{84}$) were basically immobile, with some
490 downstream rotation and imbrication observed at the Q_{50} flow at the 5% slope due to scour
491 downstream of boulders. Medium-sized sediment ($\sim D_{50}$) also showed imbrication at the Q_{10} and
492 Q_{50} flows at both slopes; imbrication was located directly upstream of large clasts or independent
493 of the hydraulic influence of boulders (Figure 4b; 4c). Most sediment transport occurred at the
494 beginning of each flow, and mobile sediment was quickly deposited in shielded or stable
495 locations, inhibiting potential further transport until the next higher discharge was run. Sediment
496 clusters of small- to medium-sized sediment ($\sim$4-20 mm), corresponding to grains sizes between
497 the D_{10} and D_{50}, were observed upstream of immobile clasts after the Q_{10} flows at both slope
498 setups, with corresponding scour downstream of immobile clasts (Figure 4). . Because the large
499 clasts remained immobile at all flows, no classic bedforms, including steps, developed in these
500 experiments; however, the formation of small-scale bedforms and structures around boulders are
501 discussed below (section 3.3).
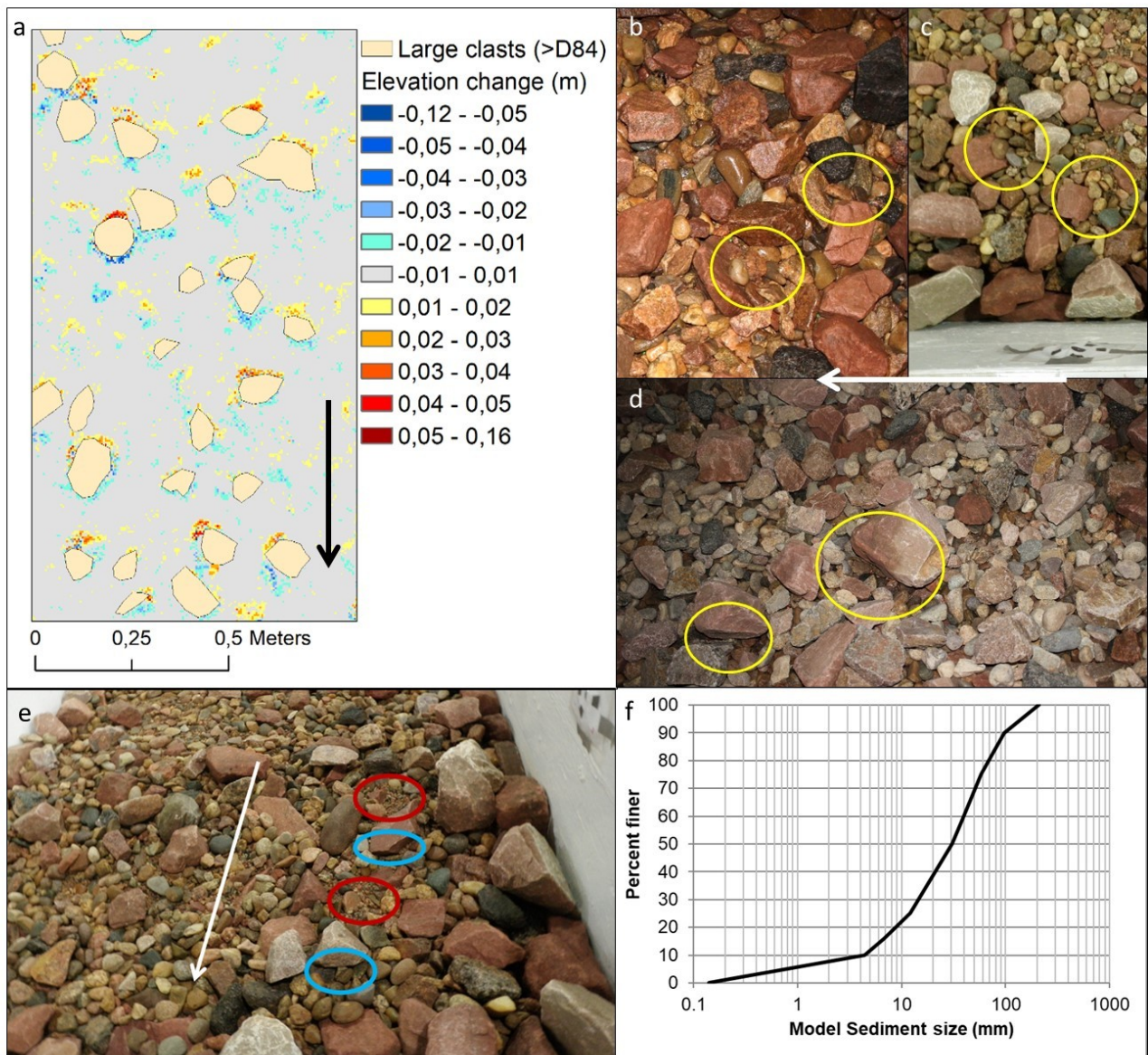
Figure 4. Patterns of erosion and sedimentation after flume runs: a) elevation change after Q_{10} flow at 2% slope setup around large clasts ($>D_{84}$). Photos (b & c) show imbrication, both after Q_{10} flow, at 5% and 2% slope setups, respectively. (d) Scour forms downstream of large clasts after Q_{50} flow at 5% slope setup, which caused slight downstream rotation of large clasts. (e) Photo after Q_{10} flow at 2% slope setup showing patterns of sedimentation (red) and scour (blue) around large clasts. (f) Sediment size distribution for flume experiments. See Polvi et al. (2014) for range of grain size distributions for enhanced (referred to as 'demo') and unimpacted reaches. Arrows indicate flow direction.

The relative submergences (RS) of large boulders ($>D_{84}$) differed for each flow but were similar between slope setups (Figure 2; Table 2); RS values were calculated for the D_{84} clast size and is therefore lower for larger clasts. At the Q_1 flow, the RS was very low (0.31 and 0.32) at both slopes; a few surface waves were evident at the 5% slope but very little turbulence or surface waves were evident at the 2% slope. At Q_2, wakes start to form downstream of boulders,

516   and the RS was ~0.6. The RS at the Q_{10} flow was approaching 1 at the 2% slope (0.87 for D_{84})
517   and ranged from ~0.8-1.2 for the 5% slope with clear boulder-affected wakes forming. At the Q_{50}
518   flow, all boulders were nearly submerged at both slopes. At the 2% slope, the RS = 1.0 and
519   waves and wakes formed downstream of boulders; at the 5% slope, the average RS was
520   calculated to be less than 1 but according to visual observations seemed to range from 1-1.5 with
521   very turbulent flow. All reach-scale Froude numbers were below 1 (Table 2), but there was
522   variation throughout the reach with local zones of critical and supercritical flow around clasts
523   >D_{84}, particularly at Q_{10} and Q_{50} flows.

524   3.2 Summary of aggradation/degradation results

525   Less than 20% (7.13- 19.91%) of the flume area was re-worked through erosion or
526   deposition (>0.01 m positive or negative elevation change) during each flow for both slope
527   setups (Table 3). At the 2% slope, 3.40-9.80% of the flume area was eroded after each flow, and
528   1.58-7.60% of the flume area experienced deposition. At the 5% slope, 4.93-10.39% of the flume
529   was eroded, and 5.85-11.26% of the flume area experienced deposition.

530   At the 2% slope, the Q_{10} flow does the most amount of work (0.044 m^3), followed closely
531   by the Q_1 flow (0.042 m^3) (Table 3). This was visually observed during the flume runs as the
532   bankfull flow was able to mobilize fine sediment. Because there was no input of fine sediment
533   during or between the runs at a given slope, by the time the highest flow (Q_{50}) was run, all
534   potentially mobilized sediment had either already been transported out of the system or settled
535   into a shielded or non-mobile position. With little available fine sediment, combined with the Q_{50}
536   flow not being competent enough to start mobilizing the large clasts (>D_{84}), the largest flow, Q_{50},
537   actually does the least amount of work (0.028 m^3). Because it would not have been possible to
538   re-create the exact same initial conditions with such a wide grain size distribution (Figure 4f), the
539   closest estimation of comparing the work by each flow from initial conditions is by calculating
540   cumulative geomorphic work. Here, the cumulative Q_{50} flow (representing the sum of work by
541   the Q_1, Q_2, Q_{10} & Q_{50} flows) eroded and deposited ~3.5 times as much sediment as the Q_1 flow
542   but only 1.2 times that of the cumulative Q_{10} flow (sum of Q_1, Q_2 & Q_{10} flows) (Table 3; Figure
543   S2).

544   At the 5% slope, the Q_{50} flow does the most amount of geomorphic work , followed in
545   descending order by the Q_1, Q_2, and Q_{10} flows. As noted by visual observations of the flume runs
546   and the DoDs, at the Q_{50} flow, the largest clasts start to mobilize by rolling slightly (due to
547   downstream scour); but the other flows show the same process as with the 2% slope, where the
548   potentially mobile sediment has already been moved. Considering cumulative geomorphic work,
549   the Q_{50} flow eroded and deposited ~3.5 times as much sediment as the Q_1 flow and 1.6 times that
550   of the Q_{10} flow at the 5% slope (Table 3; Figure S2).

551   The shear stress for the Q_1 flow at the 5% slope was roughly the same as that of the Q_{10}
552   flow at the 2% slope. At the Q_2 flow at the 5% slope, the shear stress (22.3 N/m^2) already
553   exceeded that of the shear stress at the Q_{50} flow at the 2% slope (13.36 N/ m^2) (Table 2);
554   however, the geomorphic work did not differ greatly between slopes for the same flows, likely
555   because shear stresses were not sufficient to entrain the coarser fractions even at the 5% slope
556   (Table 2). Dimensionless shear stress values for D_{50} grain sizes at the 2% slope did not exceed
557   0.027, and thus were only approximately 50% of the slope-dependent τ_c* value of 0.056 (*sensu*

558 Lamb et al. 2008) and <30% that of 0.1 (Lenzi et al. 2006b).. The same analysis for the D_{50} at the
559 5% slope results in $\tau*$ values of 0.024-0.058, which is also substantially lower than than the τ_c*-
560 value of 0.071 (*sensu* Lamb et al. 2008) or 0.1.

561 **Table 2.** Hydraulic & Shear Stress Parameters

Slope	Flow	Q (m³/s)	Stream power Ω (N/s)	Froude #	Mean flow depth (m)	Relative submergence (d/D₈₄)	τ (N/m²)	τ* for D₅₀ mobilization
2%	Q_{bf}	0.006	1.18	0.47	0.024	0.31	4.48	0.009
	Q_2	0.017	3.34	0.45	0.049	0.63	8.87	0.018
	Q_{10}	0.025	4.91	0.41	0.068	0.87	11.83	0.024
	Q_{50}	0.031	6.08	0.42	0.078	1.00	13.36	0.027
5%	Q_{bf}	0.006	2.94	0.43	0.025	0.32	11.88	0.024
	Q_2	0.017	8.34	0.45	0.050	0.64	22.30	0.044
	Q_{10}	0.025	12.26	0.51	0.058	0.75	25.91	0.052
	Q_{50}	0.031	15.21	0.52	0.067	0.856	29.20	0.058

562
563
564
565
566 **Table 3.** Erosion, deposition and geomorphic work calculations
567
568

Slope	Pre-flow	Flow	Q (m³/s)	Std. Dev. DEM (m)	Flume area with deposition (%)[a]	Flume area with erosion (%)[a]	Flume area with erosion or deposition (%)[a]	Volume of aggradation (m³)	Volume of degradation (m³)	Geomorphic work (m³)[b]	Cumulative geomorphic work (m³)[c]	Cumulative work per area (m)
		Pre		0.0228								
	Pre	Q_1	0.006	0.0231	4.83	9.80	14.63	0.013	-0.029	0.042	0.042	0.006
2%	Q_1	Q_2	0.017	0.0228	1.58	5.55	7.13	0.019	-0.017	0.036	0.079	0.011
	Q_2	Q_{10}	0.025	0.0229	7.60	7.91	15.51	0.022	-0.021	0.044	0.122	0.017
	Q_{10}	Q_{50}	0.031	0.0228	4.32	3.40	7.73	0.015	-0.013	0.028	0.150	0.021
		Pre		0.0304								
	Pre	Q_1	0.006	0.0308	5.85	7.07	12.92	0.017	-0.020	0.037	0.037	0.005
5%	Q_1	Q_2	0.017	0.0307	6.08	4.93	11.01	0.019	-0.015	0.034	0.071	0.010
	Q_2	Q_{10}	0.025	0.0306	11.26	7.48	18.74	0.006	-0.003	0.010	0.080	0.012
	Q_{10}	Q_{50}	0.031	0.0303	9.52	10.39	19.92	0.024	-0.027	0.050	0.131	0.019

[a] % area of deposition and erosion defined as area that experienced > 0.01 m net positive or negative elevation change.
[b] Geomorphic work is defined as the cumulative sum of absolute values of aggradation and degradation after each flow.
[c] Cumulative geomorphic work is defined as the sum for the given flow with all previous flows.

569

570 3.3 Erosion and deposition next to large clasts

571   Statistically significant differences in the mean elevation change of upstream and
572 downstream buffers around large clasts (>D_{84}) were found at both slope setups, and similar
573 trends were observed between each of the flows at both slopes, indicating patterns of sediment
574 organization in relation to large immobile clasts (Figure 4, 5, S3, S4). After the Q_1 flow,
575 significant degradation occurred in both the downstream and upstream buffers at the 2% slope,
576 whereas there was only significant degradation in the downstream buffer at the 5% slope. Only
577 the 5% slope showed significant differences in the upstream and downstream buffer after Q_1,
578 with more aggradation upstream. Both slope setups showed significant differences after the Q_2
579 flow with more aggradation in the downstream buffers, but at the 5% slope there was no

580 significant change in elevation in the upstream buffers. The Q_{10} flow showed significant
581 upstream buffer aggradation at both slopes and significant degradation in the downstream buffers
582 at the 2% slope. The opposite trend was evident at the Q_{50} flow at the 5% slope with degradation
583 in upstream buffers; at the 2% slope, significant, yet minimal, aggradation was found in both
584 upstream and downstream buffers.
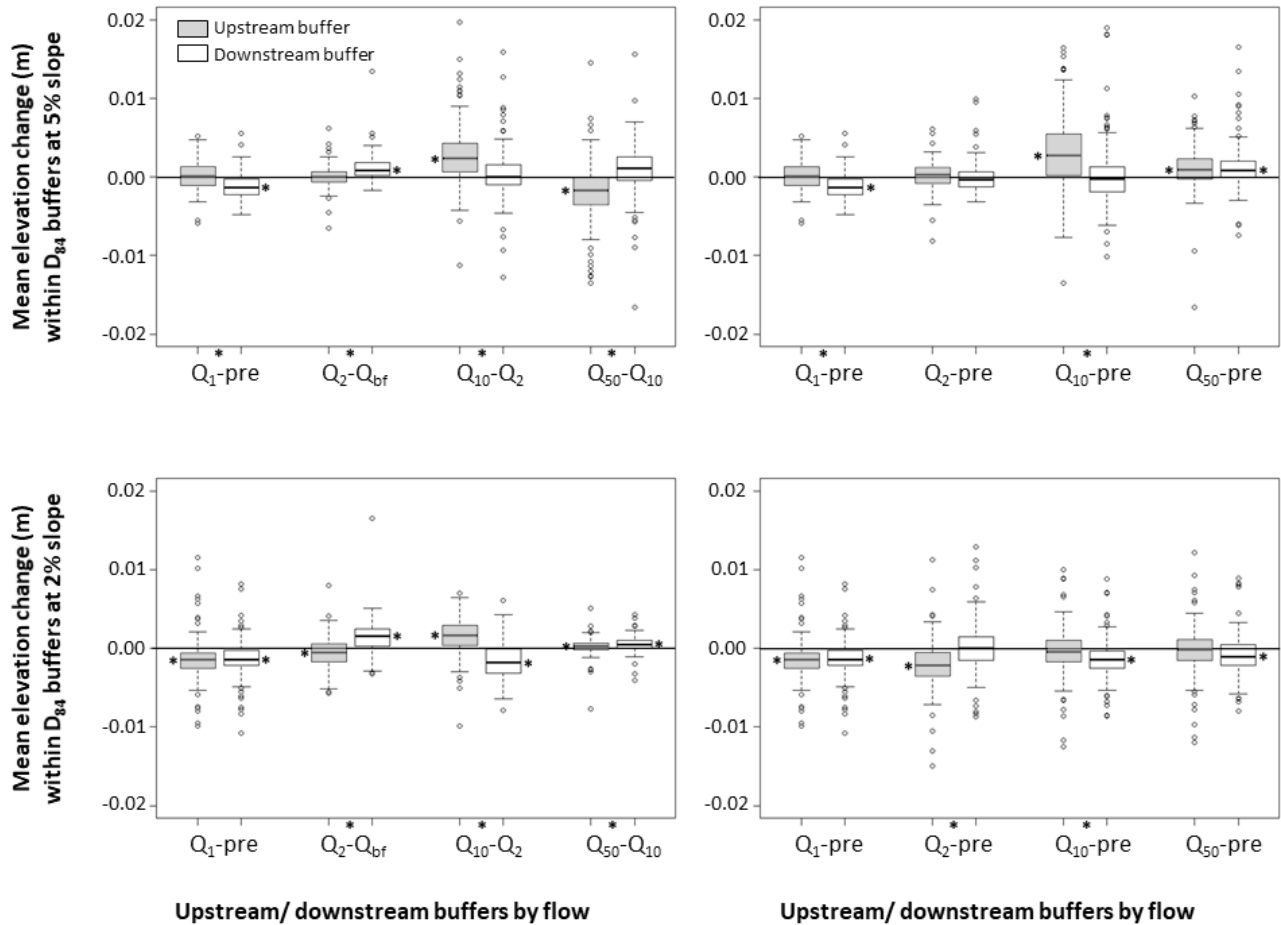
585
586 **Figure 5.** Boxplots of mean elevation change (i.e., aggradation/degradation) in buffers upstream
587 (grey) or downstream (white) of D_{84} clasts. Boxplots on left show comparisons between previous
588 flow and boxplots on right show comparisons between each flow and pre-flow conditions.
589 Asterisks next to boxplots denote that mean is significantly different from 0 at ($\alpha=0.05$) and
590 asterisks between labels on x-axis denote that there is a significant difference between the mean
591 elevation change in the upstream and downstream buffers.

592 **4 Discussion**

593 4.1 Geomorphic work and channel reworking

594   This flume experiment was designed to elucidate how semi-alluvial boulder-bed channels
595 with a snowmelt-dominated flow regime evolve in terms of potential bedforms or sediment
596 clusters. The first aspect of determining what controls channel evolution in these channels was to
597 examine whether it is possible to determine which flow is the channel-forming discharge within

598   the present flow regime. These flows were modeled with clear-water conditions, which was
599   considered representative of what these channels experience in northern Sweden. This low
600   sediment supply is due to a combination of the low sediment production in the landscape and
601   lakes along the stream network that buffer sediment coming from upstream. Therefore, the order
602   of the flows, which was from the lowest to the largest flows, played a crucial role in determining
603   how much sediment was available to be re-worked. At the 2% slope, the Q_1 flow did almost the
604   same amount of work as the Q_{10} flow (0.042 and 0.044 m^3 of combined aggradation and
605   degradation, respectively), but this is likely a function of the order the flows were conducted.
606   The Q_{50} flow did the least amount of geomorphic work at the 2% slope, because there was very
607   little mobile sediment remaining after the previous lower flows had deposited the available
608   sediment in stable locations, thus potentially increasing the critical shear stress (Masteller et al.,
609   2019). Therefore, examination of the cumulative geomorphic work for the successive flows is
610   more appropriate within this experimental setup. The cumulative geomorphic work is naturally
611   largest for the Q_{50} flow, as it has summed aggradation and degradation for previous flows;
612   however, the cumulative geomorphic work for the Q_{50} flow is only approximately three times
613   that of the Q_1 flow at the 2% flow. In channels with a broad or bimodal sediment distribution,
614   clusters tend to remain stable unless the anchor sediment is entrained during high flows
615   (Hendrick et al., 2010); therefore, once sediment clusters form at lower flows, those sediment
616   particles are more difficult to mobilize even at higher flows.

617   At the 5% slope, the Q_1 and the Q_2 flows did similar amounts of geomorphic work, which
618   was approximately three times the amount as that of the Q_{10} flow . This marked decrease in
619   sediment transport during the Q_{10} flow can be explained in a similar way to that of the Q_{50} flow at
620   the 2% slope, that all potentially mobile sediment had been mobilized and deposited in a stable
621   setting before the Q_{10} flow. The Q_{50} flow did almost two and five times the amount of
622   geomorphic work compared to the Q_2 and Q_{10} flows, respectively, at the 5% slope, but this is an
623   artefact of slight downstream rotation of large clasts, which appears as downstream
624   sedimentation and upstream degradation relative to boulders' previous positions. However, as
625   these results are dependent on the sequencing of flows, they should not be interpreted as
626   indicative of the relative amount of geomorphic work done by these flows over a longer period
627   of time with a varying sequence of flow events. Had the higher flows preceded low flows, then
628   the geomorphic work done by the lower flows would likely have been much lower. That said,
629   these results can indicate whether the larger flows are capable of resetting the channel by
630   reworking most of the bed sediment and entraining boulders. Because the Q_{50} flow did less
631   geomorphic work than the Q_1 at the 2% slope, the Q_{50} is clearly not capable of reworking the
632   channel bed. Although the Q_{50} flow did do more geomorphic work than the Q_1 flow at the 5%
633   slope, the higher amount of work is an artefact of slight rolling of large clasts and thus the Q_{50}
634   did not rework the channel bed at the higher slope either.

635   Through this flume experiment, it was only possible to test flows up to Q_{50}, due to the
636   capacity of the pump; however, we can get a sense of the magnitude of flows necessary to
637   transport boulders and re-work the channel bed. In this experiment, the geomorphic work done
638   by the Q_{50} flow may be underestimated because it was preceded by several runs with lower flows
639   that can cause interlocking of grains, thus increasing the necessary critical dimensionless shear
640   stress (Masteller et al., 2019). However, given that the Q_{50} flow did not re-work the channel more
641   than the Q_1 flow and no clasts $>D_{84}$ were transported, we can conclude that the Q_{50} flow is not
642   capable of disrupting grain interlocking in these channel types. In other steep, coarse-grained

643   channels, boulder or bedform reorganization occurs during much lower recurrence interval

644   flows; for example, step-pool structures in the Erlenbach, a small step-pool stream in

645   Switzerland (18% slope), were completely rearranged three times within a 20-year period

646   (Turowski et al., 2009). The recurrence intervals of the effective or channel-forming discharge in

647   other steep coarse-bed channels have ranged from the Q_1 to the Q_{50} flow depending on slope,

648   sediment size distribution and bedforms (Bunte et al., 2014; Hassan et al., 2014; Lenzi et al.

649   2006a), in addition to the local hydroclimatic regime controlling the magnitude of high

650   recurrence-interval flows. Results from this study indicate that these semi-alluvial rapids in

651   northern Sweden are similar to step-pool channels in alluvial, snowmelt-dominated Rocky

652   Mountain streams where low flows may do a large amount of geomorphic work, depending on

653   the history of previous flows (Bunte et al., 2014; Hassan et al., 2014). However, these low flows

654   may only reflect a channel-maintaining and not a channel-forming flow (Hassan et al., 2014).

655   That begs the question of if fairly high flows (Q_{50}) are not capable of mobilizing

656   boulders, what is the channel-forming flow and how did these channels originally form? Because

657   of the snowmelt-dominated flow regime with buffering of flows by mainstem lakes, extremely

658   high flows are unlikely (Arp et al., 2006; Bergstrand et al., 2014). The Q_{50} flow is only 1.8 times

659   that of the Q_2 flow in this experiment, and the ratio of the Q_{50} to the Q_1 in this region ranges from

660   1.5-1.9 (Bergstrand et al., 2014). If the Q_{100} and Q_{500} flows follow the same logarithmic trend,

661   those flows will only be 1.12 and 1.38 times that of the Q_{50} flow, respectively. Furthermore, the

662   prototype channels are located in partly confined to unconfined moraine-, drumlin-, or esker-

663   bounded floodplains, so flow depths would not increase significantly with higher flows. There

664   are few mechanisms for post-glacial extreme flows in streams originating below the Scandes

665   mountains in inland northern Sweden. Potential mechanisms for extreme flows, which do not

666   follow the modeled RI-Q relationships, that cannot be ruled out include local cumulative effects

667   of breached beaver dams or moraine-dammed lakes combined with a rain-on-snow event over

668   seasonally-frozen ground. Based on the low magnitude of high-recurrence interval hydrologic

669   events in this region, combined with results from this study showing that the Q_{50} flow is not

670   channel-forming, it is unclear how often channel-forming flows, that are capable of transporting

671   boulders, occur in these streams.

672   Large rivers in northern Sweden (e.g., Ume, Vindel, Lule Rivers) with steep bedrock

673   gorges, to which these semi-alluvial channels are tributaries, were formed by sub-glacial

674   meltwater while glaciers were melting ca 10,000 y. BP and have experienced very little fluvial

675   erosion post-glaciation (Jansen et al., 2014). Although this study did not model higher than Q_{50}

676   flows, there is a possibility that these semi-alluvial channels have not experienced a channel-

677   forming discharge (capable of transporting boulders) since directly pre- or post-deglaciation

678   when flow magnitudes could have been much larger and under higher pressure (Herman et al.,

679   2011) and thus competent enough to move large boulders. Dimensionless shear stresses for D_{50}

680   grains range from 0.009-0.027 at the 2% slope and 0.024-0.058 at the 5% slope (Table 2), which

681   are well below critical dimensionless shear stress values of 0.056 for 2% slopes and 0.071 for 5%

682   slopes (*sensu* Lamb et al. 2008). Given the non-linear increase in τ^*_c for larger grain sizes due to

683   protrusion effects (e.g., Ashworth & Ferguson, 1989), the dimensionless shear stress values are

684   not provided for D_{84} sediment, but can be assumed to be higher than the D50 lower than with a

685   linear increase. Assuming Lamb et al.'s (2008) slope-dependent τ_c^*-values, a flow depth of 0.14

686   m (1.8 times that of the Q_{50} flow depth) would be required just to entrain D_{50} sediment in the

687   flume at the 2% slope; at the 5% slope, a water depth of 0.07 m (1.1 times that of the Q_{50} flow

688 depth) flow would be required. If a τ_c*-value of 0.1 is assumed, which may be more appropriate
689 in low RS-settings (Lenzi et al., 2006b), then depths of 0.25 m and 0.10 m are required at the 2%
690 and 5% slopes, respectively. Due to the mostly unconfined to partly confined nature of the
691 prototype streams, reaching analogous mean flow depths (1.1-2.0m and 0.57-0.81 m,
692 respectively) would require very high magnitude flows to mobilize D_{50} sediment, let alone D_{84}-
693 sized boulders. However, during deglaciation (~9000-10000 y BP), glaciers receded very rapidly
694 at ~100 km in 100 years in the inland region below the Scandes mountains (Lundqvist, 1986;
695 Stroeven et al., 2016), with the rate varying between 200 and 1600 m yr^{-1} in the region (Stroeven
696 et al., 2016). This high deglaciation rate led to locally high discharges: modelled summer
697 discharges in sub-glacial tunnels at the ice margin during deglaciation range from 100 to 300 m^3/
698 s (Arnold & Sharp, 2002; Boulton et al., 2009). These post-glacial discharges are two orders of
699 magnitude greater than the current Q_{50} and the extrapolated Q_{100} or Q_{500} flows and would thus be
700 capable of transporting much larger clasts than current flow regimes allow. Since then, with the
701 current snowmelt-dominated flow regime buffered by lakes, hydraulic processes provide few
702 mechanisms for these channels to re-organize in terms of steps, pools or other large bedforms.

703   Another potential mechanism for localized sediment transport, including that of boulders,
704 is winter ice cover and ice break-up (Lotsari et al., 2015; Polvi et al. 2020). Although boulders
705 up to 2 m in diameter can be transported by ice during ice break-up (Lotsari et al., 2015), it is
706 unclear how important the role of sporadic, localized transport by ice is for long-term channel
707 formation (Ettema & Kempema, 2013). Therefore, channels may have inherited their overall
708 geometry from unsorted glacial sediment, yet fluvial flows and ice processes from the current
709 flow regime have likely promoted the formation of sediment clusters and control microhabitat
710 formation.

711 4.2 Bedforms and sediment clusters

712   Within the flows modelled in this flume experiment, no classic alluvial steep-channel
713 bedforms, such as step-pools, developed. Large clasts are not even transported by the Q_{50} flow,
714 although some rotation and imbrication occurred at the highest flows. Thus the large clasts create
715 fixed constrictions that the remainder of mobile sediment and potential instream wood and log
716 jams form around. Even channel morphologies of steep alluvial channels (plane bed, step-pool,
717 and cascades) are most likely controlled by the location of lateral constrictions and coarse
718 sediments (Vianello & D'Agostino, 2007), and flow convergence at channel constrictions in
719 pool-riffle channels play a major role in sediment routing and backwater development
720 (Thompson & Wohl, 2009). Therefore, it is not surprising that immobile boulders would play a
721 large role in the organization of the entire channel morphology. Thus neither Montgomery &
722 Buffington's (1997) or Palucis & Lamb's (2017) general patterns regarding correlations between
723 bedforms and slope apply in this environment. According to Montgomery & Buffington's (1997)
724 bedform scheme, step-pools form in supply-limited systems. However, the setting for the
725 prototype streams are severely transport-limited system due to the non-flashy hydrological
726 regime, where very high magnitude flows are limited due to mainstem lakes and the unconfined
727 valley geometries. Furthermore, channel widths may be too large to promote boulder jamming
728 and thus step formation (Zimmerman et al., 2010).

729   Although no channel-spanning bedforms developed, there were patterns of sediment
730 deposition and scour in relation to large clasts. These patterns are in accordance with previous

731 studies on boulder-bed channels with low relative submergence regimes, where sediment will
732 deposit upstream of large immobile boulders (Monsalve & Yager, 2017; Papanicolaou et al.,
733 2011, 2018). However, in this study, this pattern was only observed at the highest flows (Q_{10} and
734 Q_{50}) when large clasts were fully submerged but still with very low RS values (1-1.3). At lower
735 flows (Q_1 and Q_2) where large clasts protruded above the water surface elevation and fully
736 turbulent and hydraulically rough flows had not developed, more sediment deposited
737 downstream of large clasts. After the Q_{10} and Q_{50} flows at both slope setups, sediment clusters of
738 fine- to medium- sized sediment (D_{10} and D_{50}) formed upstream of large clasts. Previous flume
739 experiments have examined the role of individual boulders on sediment deposition and have
740 measured the hydraulics around large clasts in low RS, in terms of velocity, shear stress, and
741 shear stress divergence. Monsalve and Yager (2017) observed sediment deposition upstream of
742 large clasts and scour between clasts, which they explained formed as a result of negative bed
743 shear stress divergence within a medium range of shear stress magnitudes so that size-selective
744 entrainment is possible, in addition to the direction of bed shear stress vectors. Papanicolaou et
745 al. (2018) note that the reversal in depositional locations in high RS versus low RS environments
746 can be due to differences in the turbulent vortex structures and that the area or length of these
747 structures relative to clasts may affect depositional areas. Furthermore, at low RS, the Froude
748 number determines the location of sediment deposition: at subcritical flows, sediment deposits in
749 the stoss of boulders but at supercritical flows, sediment can deposit at the upstream flanks of
750 boulders (Papanicolaou et al., 2018). This pattern of upstream flank depositional zones was also
751 observed in this study at the Q_{10} flow at the 5% slope, where local areas of supercritical flow
752 with small hydraulic jumps were observed.

753   These previous flume studies of the effects of boulders in low RS regimes provide
754 valuable insights into hydraulics and mechanisms of sediment deposition around boulders in low
755 RS streams (e.g., Monsalve & Yager, 2017; Papanicolaou et al. 2011, 2018); however, in order
756 to isolate the effects of individual boulders, these experiments represented oversimplified
757 conditions than those found in the field in terms of boulder spacing and sediment size
758 distribution. This study adds several layers of complexity that more accurately reflects field
759 conditions of semi-alluvial channels by using a scaled down sediment distribution from field
760 conditions of a prototype stream (Figure 4f), rather than a bimodal bed vs. boulder sediment
761 distribution. Also, in contrast to previous studies where simple bed configurations were used,
762 with isolated flow regimes where wakes do not interfere with those of consecutive boulders,
763 boulders in this study were randomly located throughout the channel. Therefore, the data showed
764 a large range in mean aggradation/degradation upstream and downstream of large clasts, as the
765 stoss or lee side of one clast may be experiencing the effects of a proximal boulder located
766 upstream, downstream or even laterally. Although a more controlled study can yield interesting
767 data on hydraulic effects of single boulders, this study provides results that reflect the complexity
768 and variability in field conditions. Therefore, even with large variation, statistically significant
769 differences in the amount erosion/deposition around boulders can provide general trends of
770 sediment patterns around boulders. Future work should expand on the detailed hydraulic
771 measurements around boulders where large clasts are unevenly spaced, affecting one another,
772 and have a wider grain size distribution, in order to determine the length and area of turbulent
773 vortex structures around clasts (per Papanicolaou et al., 2018) and how they interact with one
774 another to determine the areas of sediment deposition relative to large clasts.

775   The protrusion of large boulders can play an important role in determining potential
776 sediment transport (Yager et al., 2007, 2012). Yager et al. (2007) found that protrusion of
777 immobile grains determines the shear stress available to transport mobile sediment. Furthermore,
778 protrusion decreases when sediment is deposited which in turn increases velocities and shear
779 stress available to transport sediment. There is insufficient data in this experiment to determine
780 whether there was a feedback in degree of protrusion, aggradation, and potential for further
781 sediment transport. However, smoothing of the longitudinal profile, visualized through increased
782 elevations upstream and downstream of protrusions suggest a decrease in protrusion (Figure S5).

783 4.3 Importance & widespread distribution of semi-alluvial channels

784   Recently, the importance of large grains in controlling processes in coarse-bed streams
785 has gained prominence in the scientific literature (e.g., Williams et al., 2019). For example,
786 MacKenzie and Eaton (2017) found that a slight increase in the D_{90} of a sediment size
787 distribution caused a four-fold decrease in sediment transport. Rather than relying on the classic
788 median grain size to determine sediment transport processes and channel morphology,
789 MacKenzie et al. (2018) encourage us to examine the mobility of the largest grains in order to
790 understand channel morphology. Similarly, Yager et al. (2018) argue that grain resistance, in
791 particular that of large boulders that protrude from the channel, serve to increase the
792 dimensionless critical shear stress so that the sediment transport threshold varies substantially
793 among streams. Given these insights into the role of large grains in shaping sediment transport
794 processes and thus channel morphology, semi-alluvial channels with abundant boulders relative
795 to their transport capacity may form quite unique morphologies compared to alluvial channels.

796   Previous work on semi-alluvial channels have focused nearly solely on those with a mix
797 of alluvial and bedrock elements, with either the channel bank or bed composed of bedrock
798 (Turowski, 2012). However, few studies have examined sediment organization in semi-alluvial
799 channels where immobile sediment reduces potential sediment transport and encourages
800 sediment cluster formation. As many fluvial geomorphic studies have been conducted in
801 temperate zones, beyond the limit of continental glaciation, or in mountain environments that are
802 usually supply-limited, the sediment transport literature has focused on alluvial channels. The
803 widespread distribution of continental glaciation-related till at northern latitudes probably means
804 that boulder-bed semi-alluvial channels may also be widespread. Systematic global mapping of
805 these channel types is lacking; however, mapping of Canadian channel types suggest that semi-
806 alluvial streams are common in large parts of the Canadian Shield (Ashmore & Church, 2001).
807 Understanding these boulder-bed semi-alluvial channels bridges previous research on semi-
808 alluvial bedrock channels or low-gradient channels cut into peat or lacustrine sediment with that
809 of steep coarse-bed channels in young mountain ranges. Even in young mountain ranges,
810 hillslope-derived blocks (>1 m) can slow the rate of channel incision (Shobe et al., 2016), and
811 thus could also be described as semi-alluvial.

812   Furthermore, at northern latitudes, mainstem lakes are widespread (Messager et al.,
813 2016). With the exception of studies on the effects of lakes on sediment size in Maine, U.S.A.
814 (Snyder et al., 2012) and the effect of lakes on downstream hydraulic geometry in Idaho, U.S.A.
815 (Arp et al., 2007), the effect of lakes on geomorphic channel dynamics is little studied. Mainstem
816 lakes buffer downstream sediment transport and will decrease the fine sediment available to be
817 re-worked in a semi-alluvial rapid reach (Arp et al., 2007; Synder et al., 2012). In Fennoscandia,

818 this decrease in available fine sediment is exacerbated by the overall low sediment yield on the
819 continental shield due to the crystalline bedrock, cold climate and generally low relief (Polvi et
820 al. 2020). These conditions that lead to low sediment yields are also common in the boreal shield
821 regions of Canada, and may translate to similar low sediment yield stream systems. Fine
822 sediment can only be recruited from channel banks and local tributary junctions. This
823 interpretation is supported by analyses of sediment yields in Canada that show that sediment
824 yield increases disproportionately with drainage area because sediment is eroded directly from
825 streambanks. This indicates that rivers are degrading and that streams are eroding through
826 Quaternary deposits of glacial sediment (Church et al. 1999). In addition to streambank
827 sediment, some prototype reaches produce additional fine sediment from pre- or interglacially
828 highly weathered bedrock or boulders of Revsunds granite (*personal observation*; *personal
829 communication*, Rolf Zale). If greater amounts of fine sediment (sand to medium gravel) were
830 available, it is possible that different patterns of deposition in relation to boulders would result.

831 4.4 Implications for restoration

832 In the past two decades, semi-alluvial rapids have been targeted for restoration, with
833 >100 million Euro being spent to improve trout and salmon habitat in Sweden and Finland (e.g.,
834 Gardeström et al., 2013); however, positive ecological results have been sparse (Nilsson et al.,
835 2015). Restoration has included increasing geomorphic complexity by adding large boulders, in
836 addition to opening side channels and removing small dams, followed by adding spawning
837 gravel downstream of boulders. However, based on the results from this flume experiment, to
838 ensure the longevity of spawning beds, spawning gravel should not always be placed in
839 downstream wakes in channels with low relative submergence regimes. In contrast to alluvial
840 channels, the channel will likely not re-organize the restored major bed elements such as coarse
841 boulders. Therefore, there is a larger burden on restoration practitioners to restore these streams
842 correctly, in terms of balancing erosion and deposition and creating appropriate microhabitats.

843 **5 Conclusions**

844 A flume experiment was designed to elucidate how semi-alluvial boulder-bed channels
845 with a snowmelt-dominated flow regime evolve in terms of potential bedforms or sediment
846 clusters. These channels have a coarse sediment distribution, resembling that of steep mountain
847 streams, but previous field observations have suggested that these channels do not form
848 bedforms found in coarse-bed alluvial channels (*sensu* Montgomery & Buffington, 1997). My
849 results confirmed that even a 50-year flow event does not reorganize bed sediment to form
850 regular bedforms. However, patterns in sediment deposition were found in relation to boulders
851 ($>D_{84}$): at moderate to high flows (Q_{10}-Q_{50}), finer sediment is deposited upstream of boulders
852 rather than in downstream wakes. Because the geomorphic work done by the Q_{50} flow, following
853 a sequence of lower flows, is less than that of the annual high-flow event (Q_1), it shows that the
854 Q_{50} flow would not be able to disrupt grain interlocking and thus re-organize bedforms or
855 boulders. This finding places these boulder-bed semi-alluvial channels in a different category
856 than mountain streams, where many step-pool channels re-organize steps every 10-50 years (e.g.,
857 Bunte et al., 2014; Turowski et al., 2009). These results lead to the conclusion that the channel
858 geometry of these semi-alluvial channels do not reflect equilibrium conditions based on the
859 current snowmelt-dominated flow regime and sediment regime. The results from this study,
860 combined with low-magnitude high-recurrence flows, due to mainstem lakes that buffer high

861 flows and unconfined channel geometry, and the history of extremely high post-glacial flows,
862 suggest that few channel-forming flows have occurred post-glaciation. Channels may instead
863 have inherited their geometry from unsorted glacial sediment that was deposited from glacial
864 meltwater sub-glacially or downstream of melting glaciers ca. 9000-10000 y. B.P.

Acknowledgments

References

880 Agisoft LLC. (2014). St. Petersburg, Russia.

882 Andrews, E. D. (1980). Effective and bankfull discharges of streams in the Yampa River Basin,
883 Colorado, and Wyoming. *Journal of Hydrology, 46*, 311–330.

885 Arnold, N., & Sharp, M. (2002). Flow variability in the Scandinavian ice sheet: modelling the
886 coupling between ice sheet flow and hydrology. *Quaternary Science Reviews, 21*, 485-502.
887 https://doi.org/10.1016/S0277-3791(01)00059-2

889 Arp, C. D., Gooseff, M. N., Baker, M. A., & Wurtsbaugh, W. (2006). Surface-water
890 hydrodyanamics and regimes of a small mountain stream-lake ecosystem. *Journal of Hydrology,
891 329*, 500-513. https://doi.org/10.1016/j.jhydrol.2006.03.006

893 Arp, C. D., Schmidth, J. C., Baker, M. A., & Myers, A. K. (2007). Stream geomorphology in a
894 mountain lake district: hydraulic geometry, sediment sources and sinks, and downstream lake
895 effects. *Earth Surface Processes and Landforms, 32*, 525-543. https://doi.org/10.1002/esp.1421

897 Ashmore, P., & Church, M. (2001). The impact of climate change on rivers and river processes
898 in Canada. *Geological Survey of Canada, Bulletin* 555, 58 pp.

900 Ashworth, P. J., & Ferguson, R. I. (1989). Size-selective entrainment of bed load in gravel bed
901 streams. *Water Resources Research, 25*, 627-634.

903   Bathurst, J. C. (2002). At-a-site variation and minimum flow resistance for mountain rivers.
904   *Journal of Hydrology, 269*, 11-26. https://doi.org/10.1016/S0022-1694(02)00191-9
905

906   Bergstrand, M., Asp, S-S., & Lindström, G. (2014). Nationwide hydrological statistics for
907   Sweden with high resolution using the hydrogical model S-HYPE. Hydrology Research, 45, 349-
908   356. https://doi.org/10.2166/nh.2013.010
909

910   Boulton, G. S., Hagdorn, M., Maillot, P. B., & Zatsepin, S. (2009). Drainage beneath ice sheets:
911   groundwater-channel coupling, and the origin of esker systems from former ice sheets.
912   *Quaternary Science Reviews, 28*, 621-638. https://doi.org/10.1016/j.quascirev.2008.05.009
913

914   Bray, D. I. (1979). Estimating average velocity in gravel-bed rivers. *Journal of the Hydraulics
915   Division- ASCE, 105*, 1103-1122.
916

917   Brummer, C. J., & Montgomery, D. R. (2003). Influence of coarse lag formation on the
918   mechanics of sediment pulse dispersion in a mountain stream, Squire Creek, North Cascades,
919   Washington, United States. *Water Resources Research, 42*(7), W07412.
920   https://doi.org/10.1029/2005WR004776
921

922   Bunte, K., Abt, S. R., Swingle, K. W., & Cenderelli, D.A. (2014). Effective discharge in Rocky
923   Mountain headwater streams. *Journal of Hydrology, 519*, 2136-2147.
924   http://dx.doi.org/10.1016/j.jhydrol.2014.09.080
925

926   Chin, A., & Wohl, E. (2005). Toward a theory for step pool in stream channels, *Progress in
927   Physical Geography: Earth and Environment, 29*, 275–296.
928   https://doi.org/10.1191/0309133305pp449ra
929

930   Church, M. (2006), Bed material transport and the morphology of alluvial river channels, *Annual
931   Review of Earth and Planetary Sciences, 34*, 325-354.
932   https://doi.org/10.1146/annurev.earth.33.092203.122721
933

934   Church, M., Ham, D., Hassan, M., & Slaymaker, O. (1999). Fluvial clastic sediment yield in
935   Canada: scaled analysis. *Canadian Journal of Earth Sciences, 36*, 1267-1280.
936

937   Church M., & Zimmerman, A. (2007). Form and stability of step−pool channels: Research
938   progress. *Water Resources Research*, 43, W03415. https://doi.org/10.1029/2006WR005037
939

940   Coulombe-Pontbriand, M., & LaPointe, M. (2004). Geomorphic controls, riffle substrate quality,
941   and spawning site selection in two semi-alluvial salmon rivers in the Gaspé Peninsula, Canada.
942   *River Research and Applications, 20*, 577-590. https://doi.org/10.1002/rra.768
943

944   Curran, J. C., & Wilcock, P. R. (2005), Characteristic dimensions of the step−pool
945   configuration: An experimental study, *Water Resoures. Research, 41*, W02030,
946   https://doi.org/10.1029/2004WR003568.

David, G. C. L., Wohl, E., Yochum, S. E. & Bledoe, B. P. (2011). Comparative analysis of bed resistance partitioning in high-gradient streams. *Water Resources Research, 47*, W07507. https://doi.org/10.1029/2010WR009540

Downs, P.W., Soar, P.J., & Taylor, A. (2016). The anatomy of effective discharge: the dynamics of coarse sediment transport revealed using continuous bedload monitoring in a gravel−bed river during a very wet year. Earth Surface Processes and Landforms, 41, 147-161. https://doi.org/10.1002/esp.3785

Emmett, W. W., & Wolman, M. G. (2001). Effective discharge and gravel-bed rivers. *Earth Surface Processes and Landforms, 26*, 1369-1380. https://doi.org/10.1002/esp.303

Ettema, R., & Kempema, E.W. (2013). Ice effects on sediment transport. In *River Ice Formation ED: Spyros, B. Pp.297-338. Published by the Committee on River Ice Processes and the Environment, Canadian Geophysical Union Hydrology Section, Edmonton, Alberta, Canada* *http://cripe.civil.ualberta.ca/*

ESRI (2017). ArcGIS Desktop: v. 10.5.1. Redlands, CA: Environmental Systems Research Institute.

Faustini , J. M., Kaufmann, P. R., Herlihy, A. T. (2009). Downstream variation in bankfull width of wadeable streams across the conterminous United States, *Geomorphology, 108*, 292-311.

Gardeström, J., Holmqvist, D., Polvi, L.E., & Nilsson, C. (2013). Demonstration restoration measures in tributaries of the Vindel River catchment. *Ecology and Society, 18*(3), 8. http://dx.doi.org/10.5751/ES-05609-180308

Gran, K.B., Finnegan, N., Johnson, A. L., Belmont, P., Wittkop, C., & Rittenour, T. 2013. Landscape evolution, valley excavation, and terrace development following abrupt postglacial base-level fall. *Geological Society of America Bulletin, 125*, 1851-1864. http://dx.doi.org/10.1130/B30772.1

Grant, G.E. 1997. Critical flow constrains flow hydraulics in mobile-bed streams: A new hypothesis. Water Resources Research, 33, 349-358. http://dx.doi.org/10.1029/96WR03134

Hassan, M. A., Brayshaw, D., Alila, Y., & Andrews, E. (2014). Effective discharge in small formerly glaciated mountain streams of British Columbia: limitations and implications. *Water Resources Research, 50*, 4440-4458. http://doi/10.1002/2013WR014529.

Hendrick, R. R., Ely, L. L, & Papanicolaou, A. N. (2010). The role of hydrologic processes and geomorphology on the morphology and evolution of sediment clusters in gravel-bed rivers. *Geomorphology, 114*, 483-496. http://doi/10.1016/j.geomorph.2009.07.018

Herman, F., Beaud, F., Champagnac, J-D., Lemieux, J-M., & Sternai, P. (2011). Glacial hydrology and erosion patterns: A mechanism for carving glacial valleys. *Earth and Planetary Science Letters, 310*(3), 498-508. http://doi/10.1016/j.epsl.2011.08.022

Hey, R. D. (1979). Flow resistance in gravel-bed rivers. Journal of the Hydraulics Division-*ASCE, 105*, 365-379.

Jansen, J. D., Codilean, A. T., Stroeven, A. P., Fabel, D., Hättestrand, C., Kleman, J., et al. (2014). Inner gorges cut by subglacial meltwater during Fennoscandian ice sheet decay. *Nature Communications 5*, 3815. https://doi/10.1038/ncomms4815

Johnson, J. P. L. 2016. Gravel threshold of motion: a state function of sediment transport disequilibrium? *Earth Surface Dynamics, 4*, 685-703. https://doi/10.5194/esurf-4-685-2016

Julien, P. Y. (2002). *River Mechanics*. Cambridge, UK: Cambridge University Press.

Lamb, M. P., Dietrich, W. E., & Venditti, J. D. (2008). Is the critical Shields stress for incipient sediment motion dependent on channel-bed slope? *Journal of Geophysical Research, 113*, F02008. https://doi:10.1029/2007JF000831

Laronne, J. B., Garcia, C., & Reid, I. (2001). Mobility of patch sediment in gravel bed streams: patch character and its implications for bedload. In M. Paul Mosley (Ed.), *Gravel-Bed Rivers V* (pp. 249-289), Wellington, New Zealand: New Zealand Hydrological Society Inc.

Leach, J. A., & Laudon, H. (2019). Headwater lakes and their influence on downstream discharge. *Limnology and Oceanography Letters, 4*, 105-112. https://doi.org/10.1002/lol2.10110

Lee, A. J., & Ferguson, R. I. 2002. Velocity and flow resistance in step-pool streams. Geomorphology, 46, 59-71. https://doi.org/10.1016/S0169-555X(02)00054-5

Lenzi, M. A. (2001), Step−pool evolution in the Rio Cordon, northeastern Italy. *Earth Surface Processes Landforms,* 26, 991−1008. https://doi.org/10.1002/esp.239

Lenzi, M. A., Mao, L., & Comiti, F. (2006a). Effective discharge for sediment transport in a mountain river: computational approaches and geomorphic effectiveness. *Journal of Hydrology, 325*, 257-276. https://doi/10.1016/j.jhydrol.2005.10.031

Lenzi, M. A., Mao, L., & Comiti, F. (2006b). When does bedload transport begin in steep boulder-bed streams? *Hydrological Processes, 20*, 3516-3533. https://doi/10.1002/hyp.6168

Leopold, L. B., & Maddock, T. (1953). The hydraulic geometry of stream channels and some physiographic characteristics. Geological Survey Professional Paper 252.

Lind, L., Alfredsen, K., Kuglerová, L., & Nilsson, C. (2016). Hydrological and thermal controls of ice formation in 25 boreal stream reaches. *Journal of Hydrology, 540*, 797–811. https://doi.org/10.1016/j.jhydrol.2016.06.053

Lindström, G., Pers, C. P., Rosberg, R., Strömqvist, J., & Arheimer, B. (2010). Development and test of the HYPE (Hydrological Predictions for the Environment) model – A water quality model for different spatial scales. *Hydrology Research, 41*(3-4), 295-319. https://doi.org/10.2166/nh.2010.007

Lotsari, E., Wang, Y.S., Kaartinen, H., Jaakola, A., Kukko, A., Vaaja, M., Hyyppa, H., Hyyppa, J., & Alho, P. (2015). Gravel transport by ice in a subarctic river from accurate laser scanning. *Geomorphology, 246*, 113-122. https://doi.org/10.1016/j.geomorph.2015.06.009

Lundqvist, J. (1986). Late Weichselian glaciation and deglaciation in Scandinavia. *Quaternary Science Reviews, 5*, 269-292.

Lvovich, M. I., Karasik, G. Y., Bratseva, N. L., Medvedeva, G. P., & Maleshko, A. V. (1991). Contemporary Intensity of the World Land Intracontinental Erosion. Moscos: USSR Academy of Sciences.

MacKenzie, L.G., & Eaton, B.C. (2017). Large grains matter: contrasting bed stability and morphodynamics during two nearly identical experiments. *Earth Surface Processes and Landforms, 42*, 1287-1295. https://10.1002/esp.4122

MacKenzie, L. G., Eaton, B. C., & Church, M. (2018). Breaking from the average: why large grains matter in gravel−bed streams. *Earth Surface Processes and Landforms, 43*, 3190-3196. https://doi.org/10.1002/esp.4465

Masteller, C. C., Finnegan, N. J., Turowski, J. M., Yager, E. M., & Rickenmann, D. (2019). History-dependent threshold for motion revealed by continuous bedload transport measurements in a steep mountain stream. *Geophysical Research Letters, 46*, 2583-2591. https://doi.org/10.1029/2018GL081325

Meshkova, L. V., Carling, P. A., & Buffin-Bélanger T. (2012). Nomenclature, Complexity, Semi-alluvial Channels and Sediment-flux-driven Bedrock Erosion, In M. Church, P. M. Biron, A. Roy (Eds.), *Gravel-bed Rivers: Processes, Tools, Environments, First Edition* (pp. 424-431). Chichester, UK: John Wiley & Sons, Ltd.

Messager M. L., Lehner B., Grill G., Nedeva I. and Schmitt O. (2016). Estimating the volume and age of water stored in global lakes using a geo-statistical approach. *Nature Communications, 7*, 13603. https://doi/10.1038/ncomms13603

Monsalve, A., & Yager, E. M. (2017). Bed surface adjustments to spatially variable flow in flow relative submergence regimes. *Water Resources Research, 53*, 9350-6367. https://doi.org/10.1002/2017WR020845

Montgomery, D. R. (1999). Process domains and the river continuum. *Journal of the American Water Resources Association, 35*(2), 397-410. https://doi/10.1111/j.1752-1688.1999.tb03598.x

Montgomery, D. R., & Buffington, J. M. (1997). Channel-reach morphology in mountain drainage basins. *Geological Society of America Bulletin, 109*(5), 596-611. https://doi/10.1130/0016-7606(1997)109<0596:CRMIMD>2.3.CO;2

Morgan, J. A., Brogan, D. J., & Nelson, P. A. (2017). Application of structure-from-motion photogrammetry in laboratory flumes. *Geomorphology*, *276*, 125-143. https://doi.org/10.1016/j.geomorph.2016.10.021

Nilsson, C., Lepori, F., Malmqvist, B., Törnlund, E., Hjerdt, N., Helfield, J.M., et al. (2005). Forecasting environmental responses to restoration of rivers used as log floatways: an interdisciplinary challenge. Ecosystems, 8, 779–800. https://doi.org/10.1007/s10021-005-0030-9

Nilsson, C., Polvi, L. E., Gardeström, J., Hasselquist, E. M., Lind, L., & Sarneel, J. M. (2015). Riparian and in-stream restoration of boreal streams and rivers: success or failure? *Ecohydrology, 8*(5), 753-764. https://doi.org/10.1002/eco.1480

Nitsche, M., Rickenmann, D., Kirchner, J. W., Turowski, J. M., & Badoux, A. (2012). Macroroughness and variations in reach-averaged flow resistance in steep mountain streams. *Water Resources Research, 48*, W12518. https://doi.org/10.1029/2012WR012091

Palucis, M.C., & Lamb, M.P. (2017). What controls channel form in steep mountain streams? *Geophysical Research Letters*, 44, 7245-7255. https://doi.org/10.1002/2017GL074198

Papanicolaou, A. N., Dermisis, D. C., & Elhakeem, M. (2011). Investigating the role of clasts on the movement of sand in gravel bed rivers. *Journal of Hydraulic Engineering, 137*(9), 871-884. https://doi.org/10.1061/(ASCE)HY.1943-7900.0000381

Papanicolaou, A. N., & Kramer, C. (2005). The role of relative submergence on cluster microtopography and bedload predictions in mountain streams. In G. Parker & M. H. Garcia (Eds.), *4th IAHR symposium on river coastal and estuarine morphodynamics RCEM 2005* (pp. 1083- 1086).Urbana, IL: Taylor and Francis.

Papanicolaou, A. N., Kramer, C. M., Tsakiris, A. G., Stoesser, T., Bomminayuni S., & Chen, Z. (2012). Effects of a fully submerged boulder within a boulder array on the mean and turbulent flow fields: implications to bedload transport. *Acta Geophysica, 60*(6), 1502-1546. https://doi/10.2478/s11600-012-0044-6

Papanicolaou, A.N., Tsakiris, A.G., Wyssmanm, M.A., & Kramer, C.M. (2018). Boulder array effects on bedload pulses and depositional patches. *Journal of Geophysical Research- Earth Surface,* 123, 2925–2953. https://doi/10.1029/2018JF004753

Phillips, C. B., & Jerolmack, D. J. (2016). Self-organization of river channels as a critical filter on climate signals. *Science 352*, 694-697. https://doi/10.1126/science.aad3348

Pike, L., Gaskin, S., & Ashmore, P. (2018). Flume tests on fluvial erosion mechanisms in till-bed channels. *Earth Surface Processes and Landforms, 43*, 259-270.

Polvi, L.E. (2020). Morphology of boulder-bed semi-alluvial channel beds: a flume study modelling streams in northern Fennoscandia. Swedish National Data Service. https://doi.org/10.5878/kz4r-6y69 (Polvi, 2020).

Polvi, L.E., Dietze, M., Lotsari, E., Turowski, J.M., & Lind, L. (2020). Seismic Monitoring of a Subarctic River: Seasonal Variations in Hydraulics, Sediment Transport, and Ice Dynamics. *Journal of Geophysical Research- Earth Surface*, 125, e2019JF005333. https://doi.org/10.1029/2019JF005333

1097 Polvi, L. E., Nilsson, C., & Hasselquist, E. M. (2014). Potential and actual geomorphic
1098 complexity of restored headwater streams in northern Sweden. *Geomorphology, 210*, 98-118.
1099 https://doi/10.1016/j.geomorph.2013.12.025

1100 Reid, I., Frostick, F.E., Layman, J.T. (1985). The incidence and nature of bedload transport
1101 during flood flows in coarse grained alluvial channels. *Earth Surface Processes and Landforms,*
1102 *10*, 33–44

1103 Reid, H. E., Brierley, G. J., Mcfarlane, K., Coleman, S. E., & Trowsdale, S. (2013). The role of
1104 landscape setting in minimizing hydrogeomorphic impacts of flow regulation. International
1105 Journal of Sediment Research 28, 149-161. https://doi.org/10.1016/S1001-6279(13)60027-X

1106 Rosenfeld, J., Hogan, D., Palm, D., Lundquist, H., Nilsson, C., & Beechie, T. J. (2011).
1107 Contrasting Landscape Influences on Sediment Supply and Stream Restoration Priorities in
1108 Northern Fennoscandia (Sweden and Finland) and Coastal British Columbia. Environmental
1109 Management, 47(1), 28-39. https://doi.org/10.1007/s00267-010-9585-0

1110 RStudio Team (2016). RStudio: Integrated Development for R, v. 1.1.383. Boston, MA:
1111 RStudio, Inc. http://www.rstudio.com/

1112 Sear, D. (1996). Sediment transport processes in pool-riffle sequences. *Earth Surface Processes*
1113 *and Landforms*, 21, 241-262. https://doi/ 10.1002/(SICI)1096-9837(199603)21:3<241::AID-
1114 SP623>3.0.CO;2-1

1115 Seppälä, M. (2005). Glacially sculptured landforms, In M. Seppälä (Ed.), *The Physical*
1116 *Geography of Fennoscandia* (pp 35- 57). New York: Oxford University Press.

1117 Shobe, C.M., Tucker, G.E., & Anderson, R.S. (2016). Hillslope-derived blocks retard river
1118 incision. *Geophysical Res. Letters, 43*, 5070-5078. https://doi.org/ 10.1002/2016GL069262

1119 SMHI (2015). Vattenwebb: S-HYPE model data. Retrieved from http://vattenwebb.smhi.se/

1120 SMHI (2017). Swedish Meteorological and Hydrological Institute. Retrieved from
1121 http://www.smhi.se

1122 Stroeven, A. P., Hättestrand, C., Kleman, J., Heyman, J., Fabel, D., Fredin, O., et al. (2016).
1123 Deglaciation of Fennoscandia. *Quaternary Science Reviews, 147*, 91-121.
1124 https://doi.org/10.1016/j.quascirev.2015.09.016

1125 Snyder, N. P., Castele, M. R., & Wright, J. R. (2008). Bedload entrainment in low-gradient
1126 paraglacial coastal rivers of Maine, U.S.A.: implications for habitat restoration. *Geomorphology*
1127 *103*, 430-446. https://doi/10.1016/j.geomorph.2008.07.013

1128 Synder, N., Nesheim, A. O., Wilkins, B. C, & Edmonds, D. A. (2012). Predicting grain size in
1129 gravel-bedded rivers using digital elevation models: application to three Maine watersheds.
1130 Geological Society of America Bulletin. https://doi/10.1130/B30694.1

Thompson, D. (2008). The influence of lee sediment behind large bed elements on bedload transport rates in supply-limited channels. *Geomorphology, 99*, 420-432. https://doi/https://doi.org/10.1016/j.geomorph.2007.12.004

Thompson, D. M., & Wohl, E. E. (2009).The linkage between velocity patterns and sediment entrainment in a forced-pool and riffle unit. *Earth Surface Processes and Landforms, 34*, 177-192. https://doi/10.1002/esp.1698

Torizzo, M., & Pitlick, J. (2004). Magnitude-frequency of bed load transport in mountain streams in Colorado. *Journal of Hydrology, 290*, 137-151. https://doi/10.1016/j.hydrol.2003.12.001

Turowski, J. M. (2012). Semi-alluvial channels and sediment-flux-driven bedrock erosion. In M. Church, P. M. Biron, A. Roy (Eds.), *Gravel-bed Rivers: Processes, Tools, Environments, First Edition* (pp. 401-416). Chichester, UK: John Wiley & Sons, Ltd.

Turowski, J. M., Yager, E. M., Badoux, A., Rickenmann, D., & Molnar, P. (2009). The impact of exceptional events on erosion, bedload transport and channel stability in a step-pool channel. *Earth Surface Processes and Landforms, 34*, 1661-1673. https://doi.org/10.1002/esp.1855

Vianello, A., & D'Agostino, V. (2007). Bankfull width and morphological units in an alpine stream of the dolomites (northern Italy). *Geomorphology, 83*, 266-281. https://doi.org/10.1016/j.geomorph.2006.02.023

Walling, D. E., & Webb, B. W., (1983). Patterns of sediment yield. In K. J. Gregory (Ed.), *Background to Palaeohydrology* (pp. 69-100). Chichester, UK: Wiley.

Westoby, M. J., Brasington J., Glasser, N. F., Hambrey, M. J., & Reynolds, J. M. (2012). 'Structure-from-Motion' photogrammetry: a low-cost, effective tool for geoscience applications. Geomorphology, 179, 300-314. https://doi.org/10.1016/j.geomorph.2012.08.021

Wheaton, J. M., Brasington, J., Darby, S. E., & Sear, D. A. (2010). Accounting for uncertainty in DEMs from repeat topographic surveys: improved sediment budgets. *Earth Surface Processes and Landforms, 35*, 136-156. https://doi/10.1002/esp.1886

Whittaker, J. G., & Jaeggi, M. N. R. (1982). Origin of step−pool systems in mountain streams, *Journal of the Hydraulic Division, ASCE, 108*, 758–773.

Williams, R. D., Reid, H. E., & Brierley, G. J. (2019). Stuck at the bar: larger-than-average grain lag deposits and the spectrum of particle mobility. *Journal of Geophysical Research- Earth Surface, 124,* 2751-2756. https://doi.org/10.1029/2019JF005137

Wolman, M. G., & Miller, J. P. (1960). Magnitude and frequency of forces in geomorphic processes. *J. Geol., 68*, 54–74.

Yager, E. M., Kirchner, J. W., & Dietrich, W. E. (2007). Calculating bed load transport in steep boulder bed channels. *Water Resources Research, 43*, W07418. https://doi.org/10.1029/2006WR005432

1167 Yager, E. M., Turowski, J. M., Rickenmann D., & McArdell, B. W. (2012). Sediment supply,
1168 grain protrusion, and bedload transport in mountain streams. *Geophysical Research Letters, 39*,
1169 L10402. https://doi.org/10.1029/2012GL051654

1170 Yager, E. M., Schmeeckle, M. W., & Badoux, A. (2018). Resistance is not futile: grain resistance
1171 controls on observed critical shields stress variations. *Journal of Geophysical Research- Earth*
1172 *Surface, 123*, 3308-3322. https://doi.org/10.1029/2018JF004817

1173 Zimmermann, A., & Church, M. (2001). Channel morphology, gradient profiles and bed stresses
1174 during flood in a step−pool channel. *Geomorphology, 40*, 311–327.
1175 https://doi.org/10.1016/S0169-555X(01)00057-5

1176 Zimmermann, A., Church, M., & Hassan, M. A. (2010). Step-pool stability: testing the jammed
1177 state hypothesis. *Journal of Geophysical Research- Earth Surface, 115*, F02008.
1178 https://doi.org/10.1029/2009JF001365

1179

1180